New Phytologist

Osa-miR160a confers broad-spectrum resistance to fungal and bacterial pathogens in rice

Qin Feng, He Wang, Xue-Mei Yang, Zhang-Wei Hu, Xin-Hui Zhou, Ling Xiang, Xiao-Yu Xiong, Xiao-Rong He, Yong Zhu, Guo-Bang Li, Jing-Hao Zhao, Yun-Peng Ji, Xiao-Hong Hu, Mei Pu, Shi-Xin Zhou, Zhi-Xue Zhao, Ji-Wei Zhang, Yan-Yan Huang, Jing Fan, Wen-Ming Wang and Yan Li

State Key Laboratory of Crop Gene Exploration and Utilization in Southwest China, Sichuan Agricultural University, Chengdu 611130, China

Authors for correspondence:
Wen-Ming Wang
Email: j316wenmingwang@sicau.edu.cn

Yan Li
Email: jiazaihy@163.com;
liyan_rice@sicau.edu.cn

Received: *14 July 2022*
Accepted: *27 August 2022*

New Phytologist (2022) **236:** 2216–2232
doi: 10.1111/nph.18491

Key words: *ARFs*, bacterial leaf blight, miR160a, rice blast, rice sheath blight, *WRKY45*.

Summary

- Rice production is threatened by multiple pathogens. Breeding cultivars with broad-spectrum disease resistance is necessary to maintain and improve crop production. Previously we found that overexpression of miR160a enhanced rice blast disease resistance. However, it is unclear whether miR160a also regulates resistance against other pathogens, and what the downstream signaling pathways are.
- Here, we demonstrate that miR160a positively regulates broad-spectrum resistance against the causative agents of blast, leaf blight and sheath blight in rice. Mutations of miR160a-targeted *Auxin Response Factors* result in different alteration of resistance conferred by miR160a. miR160a enhances disease resistance partially by suppressing *ARF8*, as mutation of *ARF8* in *MIM160* background partially restores the compromised resistance resulting from MIM160.
- ARF8 protein binds directly to the promoter and suppresses the expression of *WRKY45*, which acts as a positive regulator of rice immunity. Mutation of *WRKY45* compromises the enhanced blast resistance and bacterial leaf blight resistance conferred by *arf8* mutant.
- Overall, our results reveal that a microRNA coordinates rice broad-spectrum disease resistance by suppressing multiple target genes that play different roles in disease resistance, and uncover a new regulatory pathway mediated by the miR160a-*ARF8* module. These findings provide new resources to potentially improve disease resistance for breeding in rice.

Introduction

Rice is a staple food feeding half of the world's population (Elert, 2014). However, rice production is threatened by devastating diseases worldwide, such as rice blast, sheath blight and bacterial leaf blight. Rice blast, caused by the seminecrotrophic fungal pathogen *Magnaporthe oryzae*, occurs throughout the whole growth period. Sheath blight, caused by the necrotrophic fungal pathogen *Rhizoctonia solani*, occurs on sheaths and leaves. Bacterial leaf blight is caused by the bacterial pathogen *Xanthomonas oryzae* pv *oryzae* (*Xoo*) mainly on leaves (Lee & Rush, 1983; Gnanamanickam *et al.*, 1999; Talbot, 2003).

To counter disease challenge, plants have developed a multiple-layer immune system to defend against pathogens. This immune system is mostly composed of proteins, but also includes RNA components. In particular, microRNAs (miRNAs) have recently been identified as important regulators in plant defenses against biotic stresses, including pathogens (Song *et al.*, 2019). MicroRNAs are a class of endogenous small noncoding RNAs that suppress expression of target genes via DNA methylation, mRNA cleavage or translational inhibition after binding their target DNA or RNA sites (Voinnet, 2009; Fabian *et al.*, 2010). A series of miRNAs have been characterized as immune regulators in rice in response to multiple pathogens (Li *et al.*, 2014; Lian *et al.*, 2016; Lin *et al.*, 2016; W. Q. Li *et al.*, 2018; Jia *et al.*, 2020). For example, 13 miRNAs act as negative regulators of rice blast disease resistance, including miR156 (Zhang *et al.*, 2020), miR164a (Z. Wang *et al.*, 2018), miR167d (Zhao *et al.*, 2020), miR168 (Wang *et al.*, 2021), miR169 (Y. Li *et al.*, 2017), miR1871 (Li *et al.*, 2022a), miR1873 (Zhou *et al.*, 2020), miR319 (Zhang *et al.*, 2018), miR439 (Lu *et al.*, 2021), miR1432 (Li *et al.*, 2021b), miR396 (Chandran *et al.*, 2018), miR530 (Li *et al.*, 2021a) and miR535 (Zhang *et al.*, 2022). By contrast, seven miRNAs play a positive role in rice immunity against *M. oryzae* by suppressing their target genes, including miR7695 (Campo *et al.*, 2013), miR166h-166k (Salvador-Guirao *et al.*, 2018), miR398b (Y. Li *et al.*, 2019), miR162a (Li *et al.*, 2020), miR159a (Chen *et al.*, 2021), miR171b (Li *et al.*, 2022b) and miR812w (Campo *et al.*, 2021). Besides, several miRNAs were characterized as regulators

of rice resistance against other pathogens in rice. miR156 negatively regulates rice resistance against *Xoo* by promoting the gibberellic acid (GA) signaling pathway (Liu *et al.*, 2019). miR444 enhances defense responses against rice stripe virus (RSV) through promoting expression of *RDR1* which acts as a key component of the antiviral RNA-silencing pathway (Wang *et al.*, 2016). miR528 promotes RSV colonization via reducing reactive oxygen species (ROS) production (Wu *et al.*, 2017). miR396 negatively regulates resistance to *Dickeya zeae*, the agent causing rice foot rot disease (W. Li *et al.*, 2019).

miR160 is a conserved miRNA family targeting *Auxin Response Factors* (*ARFs*) that function as DNA-binding transcription factors in both dicots and monocots (Rhoades *et al.*, 2002). In *Arabidopsis*, miR160a is responsive to elicitor flg22, a peptide derived from well-known pathogen-associated molecular pattern (PAMP) flagellin, which induces PAMP-triggered immunity (PTI) (Li *et al.*, 2010). Moreover, transgenic lines overexpressing miR160a showed enhanced callose deposition following flg22 treatment, indicating a role in plant basal defense (Li *et al.*, 2010). In rice, three mature miR160 sequences, with one nucleotide different from one another targeting several *ARFs*, are derived from six *MIR160* loci (www.mirbase.org) (Wu *et al.*, 2009; Li *et al.*, 2014; Huang *et al.*, 2016). Small RNA-seq data revealed that miR160a was responsive to *M. oryzae* infection and accumulated in both susceptible and resistant cultivars. Overexpression of miR160a led to enhanced blast disease resistance in an *indica* cv Kasalath (Li *et al.*, 2014). These results reveal an important role for miR160a in rice immunity. However, it remains unclear whether miR160a regulates resistance against other pathogens in rice, and what its downstream signaling pathways are.

WRKY proteins are a superfamily of transcription factors regulating multiple developmental and immune activities in plants (Rushton *et al.*, 2010). In rice, several WRKY proteins regulate rice defense responses against *M. oryzae*, *Xoo* and *R. solani* (Wang *et al.*, 2015; Liu *et al.*, 2018; John Lilly & Subramanian, 2019). Specifically, *WRKY45* is one of the most well-studied family members in rice–*M. oryzae* interaction. *WRKY45* knockdown resulted in compromised resistance (Shimono *et al.*, 2007, 2012). Besides, *WRKY45* is essential for resistance mediated by Panicle blast 1 (Pb1), a coiled-coil-nucleotide-binding site-leucine-rich protein and Ideal Plant Architecture 1 (IPA1) against *M. oryzae* (Inoue *et al.*, 2013; J. Wang *et al.*, 2018). In turn, *WRKY45* is targeted and suppressed by the *M. oryzae* proteins Host Transcription Reprogramming 1 and 2 (Kim *et al.*, 2020). These studies suggested a vital role for *WRKY45* in rice–*M. oryzae* interaction.

Here, we explored the role of miR160a and its downstream signaling pathways in regulation of disease resistance to multiple pathogens in rice. We constructed transgenic lines expressing a target mimic of miR160a to block miR160a function (*MIM160*), mutated miR160a target gene *ARFs*, created double mutant *wrky45*/*arf8*, and expressed *MIM160* in *arf8*. We tested resistance of these lines to the pathogens causing the most serious rice diseases and related defense responses. Moreover, we explored downstream factors of the miR160a-*ARF8* module. Our results revealed that miR160a regulates broad-spectrum resistance in rice via suppressing its target genes which play different roles in disease resistance. Moreover, ARF8 protein plays a key role in miR160a-mediated broad-spectrum disease resistance by directly binding to the promoter and suppressing the expression of *WRKY45*, an important regulator of disease resistance in rice. Our results provide possible broad-spectrum resistance genes for rice breeding.

Materials and Methods

Plant materials and growth conditions

All the plant materials are stored in laboratory stock. Rice (*Oryza sativa* L.) *japonica* cvs Nipponbare (NPB), Taipei309 (TP309), Lijiang xin Tuan Heigu (LTH), kitaake (Kit) and *indica* cv Shuhui882 (SH882) were used in this study. Rice plants were grown in a glasshouse at 28 ± 2°C and 70% relative humidity under 12 h : 12 h, light : dark cycles, or grown in a paddy yard in Wenjiang, Chengdu, China, during the normal rice growing season from mid-April to mid-September.

Plasmid construction and genetic transformation

Transgenic lines overexpressing miR160a (*OX160a*) were constructed following a previous report (Li *et al.*, 2014). To construct *MIM160*, a 243 bp fragment including the endogenous target mimicry sequence of miR160a (chr3:6880244.0.6880486) (Seo *et al.*, 2013) was amplified from NPB genomic DNA and cloned into binary vector 35S-pCAMBIA1300. To overexpress *ARF8* or enhanced yellow florescence protein-fused *ARF8* (*eYFP-ARF8*), a full-length *ARF8* coding sequence was amplified from NPB cDNA and cloned into binary vector pCAMBIA1300-35S or pCAMBIA1300-35S:eYFP. *Agrobacterium*-mediated transformation was used to generate transgenic plants.

CRISPR/Cas9 plasmid construction and mutant screen

The CRISPR (clustered regularly interspaced short palindromic repeats)/Cas9 plasmids were constructed as previously reported (Xie *et al.*, 2015). The guide RNA (gRNA) sequences listed in Table S1 were screened by the Cas-OFF inder system (http://www.rgenome.net/cas-offinder/) to avoid potential off-target sites with the screen parameters to allow less than three base-pair mismatches and one DNA/RNA bulge. In brief, to construct the plasmids, the gRNA primers F and R were annealed to generate the gRNA fragment containing sticky ends for cloning. Then the gRNA fragment was inserted into the clone site of the pRGEB32 vector with T4 DNA ligase (NEB, Beijing, China). The vector was transformed into *Agrobacterium* strain *EHA105* for rice transformation. To generate *wrky45*/*arf8* double mutants, we first generated *arf8* mutants. A T2 homozygous knockout mutant line, *arf8-1*, which lacked the CRISPR/Cas9 insertion, was used as the background to mutate *WRKY45* using the CRISPR/Cas9 technology. To generate *MIM160*/*arf8* double mutants, we crossed *arf8-1* to *MIM160-1* plants and obtained homozygous plants at F_2. To identify the mutation sites and the existence of MIM160, the genomic DNA of transgenic plants was extracted using the CTAB method and

amplified using primers flanking the designed target site and MIM160 sequence (Table S2). The PCR products (300–500 bp) were sequenced and aligned with the wild-type (WT) genome sequence to identify the mutation sites.

Reverse-transcription quantitative polymerase chain reaction (RT-qPCR)

Three-leaf-stage rice seedlings were spray-inoculated with or without *M. oryzae* at a concentration of 1×10^5 spores ml^{-1}, and the samples were collected at indicated time points. Total RNA was extracted using the TRIzol reagent (Invitrogen) and 1 μg RNA was reverse-transcribed to cDNA using the PrimeScript™ RT reagent Kit with gDNA Eraser following the manufacturer's instruction (TaKaRa Biotechnology, Dalian, China). Reverse-transcription-qPCR was performed using SYBR Green mix (QuantiNova SYBR Green PCR Kit; Qiagen) with the indicated primers (Table S2). Rice *Ubiquitin-1* (*UBQ*) gene was selected as an internal reference for the expressed genes to normalize data. miR160a amounts were measured by STEM-LOOP qRT-PCR. Rice *U6* was selected as an internal reference to normalize the amounts of miR160a. Data were analyzed with the SPSS software using a one-way ANOVA followed by Tukey analysis with significant differences at $P < 0.05$, or two-sided Student's *t*-test with significant differences at $P < 0.05$.

Dual-luciferase reporter system

The 1.5 kb DNA sequences before the transcription start site of *WRKY45* was selected as the promoter to express firefly *luciferase* (*F-LUC*) and cloned into binary vector pCAMBIA1300 (P1300-P_{WRKY45}:*F-LUC*) with specific primers (Table S2) via homologous recombination (ClonExpress® II One Step Cloning Kit; Vazyme, Nanjing, China). Then the plasmid was introduced into *Agrobacterium* strain GV3101 via chemical conversion. An *Agrobacterium* strain expressing *35S*-promoted Rellina luciferase (*R-LUC*) was used as an internal reference to normalize the transfection efficiency. The *Agrobacterium* strains were cultured in LB at 28°C overnight and resuspended in buffer (10 mM MES, pH = 5.5–5.7; 10 mM $MgCl_2$; 200 μM acetosyringone) for infection. Images were collected at 40 h after inoculation. Leaves were sprayed with 0.5 mM luciferin containing 0.01% silwet 77 for imaging. The intensity of firefly luminescence was detected by a low-light cooled charge-coupled device imaging apparatus (Bio-Rad). The relative intensity of firefly luminescence were normalized to the Renilla luminescence intensity by a dual-luciferase reporter Kit (Beyotime, Shanghai, China) using a Glo-Max96 Microplate Luminometer (Promega) following the manufacturer's instructions.

Pathogen infection and microscopic observation

To analyze rice resistance against *M. oryzae*, the isolates (Zhong1, DZ96 and 97-27-2) were incubated in complete medium at 28°C with 12 h : 12 h, light : dark cycles for sporulation. After 2 wk, spores were collected and adjusted to $1–5 \times 10^5$ spores ml^{-1} for punch or spray inoculation. Disease lesions were captured at 5–8 d post-inoculation (dpi) and fungal biomass was measured as previously reported (Park *et al.*, 2012). In brief, the relative fungal biomass was calculated using *M. oryzae Pot2* DNA against rice ubiquitin DNA by quantitative PCR.

The *Xoo* isolate PXO99 was used to test rice leaf bright disease resistance. PXO99 was activated on TSA medium for 48 h and suspended in sterile water to $OD_{600} = 1$ for inoculation. Leaves at tillering stage were cut at leaf tips by scissors covered with bacteria solution. After 14 d, all inoculated leaves were harvested, and lesions were measured and analyzed statistically.

Rhizoctonia solani isolate AG-1-IA was used to assess rice sheath blight disease resistance. AG-1-IA was cultivated in potato dextrose agar medium for 2 d and cut into same-size circles for inoculation. Leaves at tillering stage were collected for inoculation in a laboratory. Small lumps of mycelium were placed in the middle of the leaves at high-humidity conditions at 26°C for 2–4 d. Lesions on inoculated leaves were measured using IMAGEJ for statistical analysis. To obtain the disease symptom on rice leaf sheath, the related rice lines were planted in a nursery yard in Wenjiang during the normal rice growing season from mid-April to mid-September.

H_2O_2 staining with 3,3′-diaminobenzidine (DAB)

We collected leaves of three-leaf-stage plants at 48 h after spray-inoculation with *M. oryzae* for H_2O_2 staining. DAB (Sigma Aldrich) was used as an indicator. In brief, leaves were collected and submerged into 0.5 mg ml^{-1} DAB solution and stained overnight. Next, the samples were destained with 95% alcohol at 65°C to decolor the Chl. Then the decolored samples were observed and pictured by a fluorescence microscope (Zeiss Axio Imager A2) or a stereomicroscope (SZX16; Olympus, Tokyo, Japan).

Callose deposition assay

The first leaves of 8-d-old seedlings were collected for detection of callose deposition with or without chitin induction. The leaves were harvested and vacuumed for 30 min in a solution containing 20 μg ml^{-1} chitin or in the double-distilled water (ddH_2O) and then immersed overnight. The immersed leaves were fixed in ethanol : acetic acid (3 : 1, v/v) solution for 5 h at 65°C to decolor the Chl. Then the leaves were rehydrated in 70% ethanol at 65°C for 2 h, 50% ethanol at 65°C for 2 h, and in water overnight. Next, the leaves were washed with water for three times and treated with 10% NaOH for 1 h till transparent. After being washed four times with water, the leaves were incubated in aniline blue buffer (150 mM K_2HPO_4, pH = 9.5; 0.01% aniline blue) for 4 h to stain the callose. The stained leaves were observed and pictured under a fluorescence microscope (Zeiss Axio Imager A2).

ROS burst assay

We examined the production of ROS using *Nicotiana benthamiana* leaves expressing miR160a, miR160a plus MIM160, *ARF8*

and miR160a plus *ARF8* at 40 h after infection, respectively. Leaf strips were cut into 3 × 3 mm^2 squares with three scrapes and incubated in 200 µl ddH_2O in a 96-well plate overnight to eliminate basal ROS elicited by damage. Then, the strips were treated with 20 µg ml^{-1} chitin in 200 µl reaction buffer (20 mM luminol, 10 µg ml^{-1} horseradish peroxidase (Sigma-Aldrich)). Data were collected as relative luminescence units using a GloMax96 Microplate Luminometer (Promega) for more than 30 min.

Electrophoretic mobility shift assay (EMSA)

The biotin-labeled probes were prepared as described in the instructions for the EMSA Probe Biotin Labeling Kit (Beyotime). Generally, we firstly amplified the unlabeled fragments with specific primers (Table S3) and purified the PCR products using a kit (FastPure^R Gel DNA Extraction Mini Kit; Vazyme). The purified PCR products were denatured at 95°C for 2 min to create single-stranded DNA fragments. These fragments were incubated with biotin-11-dUTP at 37°C for 30 min to obtain biotin-labeled single-stranded probes. The labeled probes were then renatured to double-stranded probes following the manufacturer's instructions (EMSA Probe Biotin Labeling Kit; Beyotime).

For the binding assay, the purified MBP-ARF8 protein was incubated with 0.5 µM specific probes in binding buffer (10 mM Tris, 0.2 mM EDTA, 20 mM KCl, 1% glycerol, 0.02% TritonX-100, LightShift Poly (dI-dC; Invitrogen)). For the competition assay, 2–4 µM competitors or cold competitors were added to the reaction. The samples were incubated at 25°C for 20 min. Then the reaction mixtures were separated via a 6% native polyacrylamide gel and transferred to a nylon membrane (Amersham Hybond^{TM}-N^+; GE, Chengdu, China). Later steps followed the instructions of the Chemiluminescent EMSA Kit (Beyotime). Luminescence intensity was detected by using a low-light cooled charge-coupled device imaging apparatus.

In vitro chromatin immunoprecipitation (ChIP)-qPCR

The experiment was conducted as previously described (W. Li *et al.*, 2017) with some modifications. Generally, we sonicated the DNA (1 µg µl^{-1}) into 400–1000 bp fragments and added a 500 µl DNA sample to 500 µl F-buffer (50 mM Tris–HCl, pH = 8.0, 1 mM EDTA, 100 mM KCl, 5% glycerol, 0.1% Triton, 100 mM dithiothreitol) containing purified MBP-ARF8 or MBP protein. The DNA–protein mixture was incubated at 4°C overnight, and then 50 µl of prewashed amylose resins (Sangon Biotech, Shanghai, China) were added to the solution and incubated at 4°C for 4 h. We collected the resins by spinning at 1000 ***g*** for 5 min at 4°C and washed the resins five times with F-buffer. The resins were resuspended in 500 µl F-buffer, and 20 µl NaCl (5 M) was added to the solution and incubated for 4 h at 65°C to dissociate the crosslinking between the DNA and proteins. We added 1 ml phenol : trichloromethane : isopentanol (25 : 24 : 1, v/v/v) to the dissociated solution to extract DNA, adjusted the DNA concentration to 10 ng µl^{-1}, and used it as the template for qPCR. All primer sequences were listed in Table S2.

Rice protoplast isolation and transfection

We conducted rice protoplast transfection following a previous report (He *et al.*, 2016). In brief, the 14-d-old etiolated rice seedlings were used to collect protoplasts. The seedings were cut into *c.* 0.5 mm strips and put into the enzyme solution (1.5% cellulase, 0.3% macerozyme, 0.4 M mannitol, 2 mM MES, 0.1× W5 buffer). The sample was first vacuumized for 30 min and then incubated for 4 h in the dark at 40 rpm and 28°C. Then the enzyme solution was removed carefully, and the tissues were resuspended in W5 buffer (154 mM NaCl, 125 mM $CaCl_2$, 5 mM KCl, 2 mM MES, pH = 5.7) and shaken gently at 80 rpm for 1 h to release protoplasts. After been filtered and washed with W5 buffer, the protoplasts were collected by centrifuging at 4°C, 200 ***g*** for 10 min. The protoplasts were washed with W5 buffer.

For transformation analysis, we mixed 2–5 µg plasmid DNA with 200 µl protoplast (2 × 10^6 cells ml^{-1}) and 200 µl PEG4000 solution (40% PEG4000, 0.4 M mannitol, 100 mM $Ca(NO_3)_2$, pH = 5.7) gently. Next, the mixture was incubated at room temperature for transformation. After 20 min, the transformation was stopped by addition of 1 ml W5 buffer. After washing with W5 buffer once, the protoplasts were resuspended with 1 ml W5 buffer and incubated at 28°C for 14–24 h. The image was captured by the fluorescence microscope (Zeiss Axio Imager A2).

Results

Overexpression of miR160a enhances broad-spectrum resistance to multiple pathogens in rice

In a previous study, we overexpressed miR160a in an *indica* cv Kasalath and found that the transgenic lines displayed enhanced resistance to blast pathogen *M. oryzae* (Li *et al.*, 2014). In this study, we aimed to explore whether and how miR160a regulates broad-spectrum disease resistance in rice. We first examined the expression patterns of miR160a in NPB background following infection by the causative agents of rice blast disease, leaf blight disease and sheath blight disease individually (Fig. S1a). The three pathogens all induced the accumulation of miR160a (Fig. S1b–d), suggesting that miR160a is responsive to the three pathogens and plays a role in the regulation of broad-spectrum resistance in rice.

We then constructed transgenic lines blocking miR160 function by expressing a target mimic (*MIM160*; Wu *et al.*, 2013) and lines overexpressing miR160a (*OX160a*) in the *japonica* cv NPB (Fig. S2a). We first analyzed the broad-spectrum disease resistance of these lines. We inoculated these lines with pathogens *M. oryzae* isolates Zhong1, 97-27-2, DZ96, *Xoo* isolate PXO99 and *R. solani* isolate AG-1-IA. Compared with the NPB control, *OX160a* plants showed a 50% or greater reduction in disease lesion size or length and supported less pathogen growth, displaying significantly enhanced resistance to all the pathogens (Figs 1a–f, S3a,b). Conversely, *MIM160* plants exhibited bigger or longer (up to *c.* 50% longer) disease lesions and supported more pathogen growth (Figs 1a–f, S3a,b). These data

demonstrate that miR160a positively regulates broad-spectrum resistance against the causative agents of the most serious rice diseases.

miR160a-targeted *ARFs* regulate broad-spectrum resistance in rice

MicroRNAs regulate development or stress responses by suppressing the expression of their target genes (Song *et al.*, 2019). In rice, five genes encoding *ARF* transcription factors have been identified as the targets of miR160a, namely *ARF8* (*Os02g41800*), *ARF10* (*Os04g43910*), *ARF13* (*Os10g59430*), *ARF18* (*Os06g47150*) and *ARF22* (*Os10g33940*; Wu *et al.*, 2009; Huang *et al.*, 2016; Fig. S2b). The mRNA concentrations of these *ARFs*, except *ARF13*, were decreased in *OX160a* lines in comparison with the NPB control, but significantly elevated in *MIM160* plants (Fig. S2c), suggesting that miR160a suppresses the four *ARFs*. We then examined their mRNA concentrations in rice leaves and found that *ARF8* was the most abundant one (Fig. S2d; Methods S1). To determine the cleavage site on *ARF* mRNAs targeted by miR160a, we mapped the directed cut site in *ARF8* mRNA using the 5′ RNA ligase-mediated rapid amplification of cDNA ends (5′ RLM-RACE) technique in *OX160a* plants and found that the cleavage occurred between the eighth and ninth bases of the predicted binding site (Fig. S2e), indicating the cleavage of *ARF8 in vivo*.

To detect whether these *ARFs* were involved in miR160a-regulated broad-spectrum disease resistance in rice, we generated mutants for all four *ARFs* using the CRISPR/Cas9 technology. We obtained two homozygous mutants for each *ARF* gene. *arf8-1* carried a one-base deletion, creating a stop codon prematurely truncating the ARF8 protein; *arf8-2* carried a six-base deletion, leading to a two-amino-acid (isoleucine and tyrosine) deletion at the DNA-binding domain after aa172 that likely affects DNA-binding activity (Fig. S4a,b). The homozygous mutants of *ARF10*, *ARF18* and *ARF22* carried deletions or insertions resulting in early stop codon or truncated protein, as listed in Fig. S4c–e. We examined the resistance of these mutants to the three pathogens. Both *arf22* and *arf18* were more resistant to *M. oryzae* and *Xoo* than was the NPB control, whereas *arf18* was more sensitive to *R. solani*, and

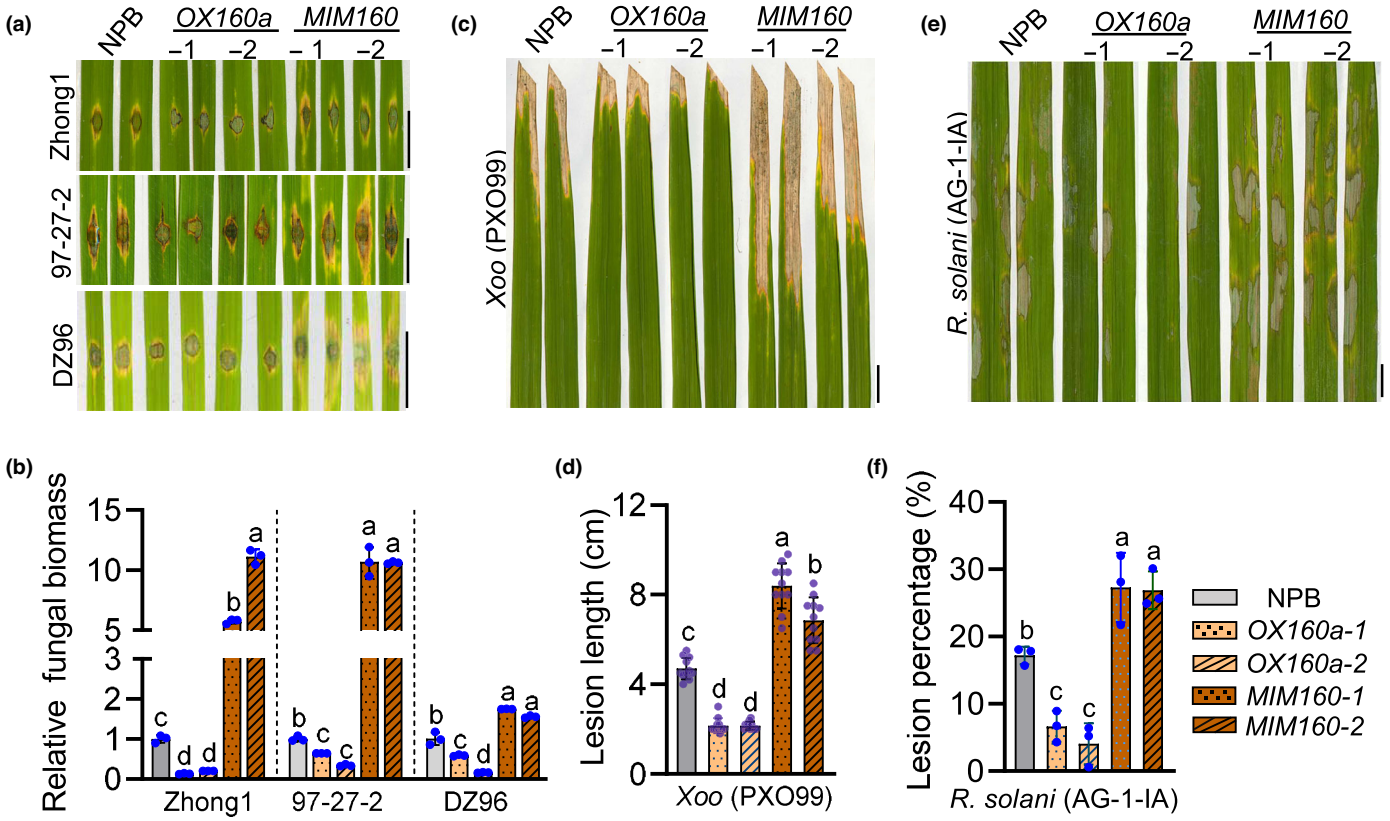

Fig. 1 miR160a positively regulates broad-spectrum disease resistance in rice. (a) Disease symptoms of miR160a overexpression lines (*OX160a*), miR160a mimic lines (*MIM160*), and the Nipponbare (NPB) controlat 7 d post-inoculation (dpi) with *Magnaporthe oryzae* isolates Zhong1, 97-27-2 and DZ96. Bar, 1 cm. (b) Fungal biomass of *M. oryzae* isolates in the indicated lines. Fungal biomass was examined by quantitative polymerase chain reaction (qPCR) and shown as the ratio of *M. oryzae MoPot2* DNA amounts against rice *ubiquitin* DNA amounts. Data are shown as means ± SD ($n = 3$). (c) Disease symptoms of the indicated lines at 14 dpi with *Xanthomonas oryzae* pv *oryzae* (*Xoo*) isolate PXO99. Bar, 1 cm. (d) Quantitative lesion lengths measured at 14 dpi as in (c). Data are shown as means ± SD ($n = 11$). (e) Disease symptoms of the indicated lines at 3 dpi with *Rhizoctonia solani* isolate AG-1-IA. Bar, 1 cm. (f) Quantitative lesion areas measured at 3 dpi as in (e). The percentages of lesion area were calculated as the ratio of lesion area to the leaf area. Data are shown as means ± SD ($n = 3$). In (b, d, f), the different letters above bars indicate significant differences at $P < 0.05$ determined by one-way ANOVA followed by *post hoc* Tukey honestly significant difference analysis, and the colored dots associated with the bars indicate the value of biologically independent samples.

arf22 displayed similar resistance to the control (Fig. 2a–f). Conversely, *arf10* exhibited more serious disease symptoms than the TP309 control following *M. oryzae* and *Xoo* inoculation, and a similar disease symptom to the control following *R. solani* inoculation (Fig. 2a–f). By contrast, the broad-spectrum resistance of *arf8* to all three pathogens was similar to that of *OX160a*, including enhanced resistance to *M. oryzae* isolates with smaller disease lesions and decreased fungal biomass, to the *Xoo* strain PXO99 with shorter disease lesions, and to the *R. solani* strain AG-1-1A with fewer disease lesions in comparison with the NPB control (Fig. 3a–f). These results indicate that miR160a enhances broad-spectrum resistance in rice by coordinately suppressing the four *ARFs* that play different roles in the regulation of immunity against different pathogens, and that *ARF8* possibly plays a key role in miR160a-mediated disease resistance.

miR160a regulates broad-spectrum disease resistance in rice partially by suppressing *ARF8*

We next further assessed the role of *ARF8* in broad-spectrum disease resistance by constructing transgenic lines overexpressing *ARF8* (*OXARF8*). We selected two independent lines, namely *OXARF8-3* and *OXARF8-13*, that showed elevated *ARF8* expression for further studies (Fig. S4f). In contrast to *arf8* lines, *OXARF8* lines showed higher susceptibility to *M. oryzae*, *R. solani* (AG-1-IA) and *Xoo* (PXO99; Figs 3a–f, S3a–c), harboring more pathogen biomass and developing bigger lesions compared with the control plants. Moreover, *OXARF8* plants displayed a severe sheath blight disease phenotype in a rice field (Fig. S3d). Collectively, these results confirm that *ARF8* plays a negative role in suppressing broad-spectrum disease resistance.

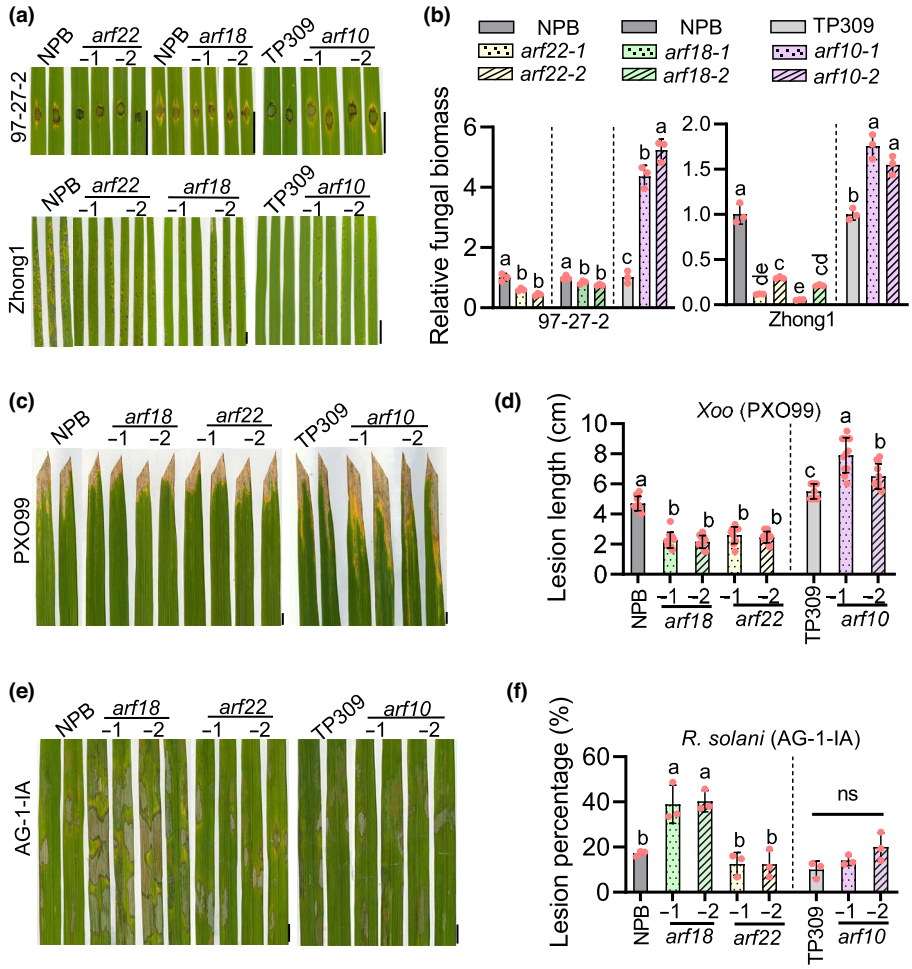

Fig. 2 miR160a-targeted *ARFs* are involved and play different roles in regulation of broad-spectrum disease resistance in rice. (a) Disease symptoms of the *Auxin Response Factor* (*ARF*) mutants and the controls (Nipponbare (NPB) and TP309) at 7 d post-inoculation (dpi) with *Magnaporthe oryzae* isolates Zhong1 and 97-27-2. Bar, 1 cm. (b) Fungal biomass of *M. oryzae* isolates in the leaves of the indicated *arf* lines and the controls in (a). Fungal biomass was determined by quantitative polymerase chain reaction (qPCR) using *M. oryzae MoPot2* DNA amounts against rice *ubiquitin* DNA amounts. Data are shown as means ± SD ($n = 3$). (c) Bacterial leaf blight disease symptoms of the indicated *arf* lines and the controls at 14 dpi with *Xanthomonas oryzae* pv *oryzae* (*Xoo*) isolate PXO99. Bar, 1 cm. (d) Quantitative lesion lengths in the inoculated leaves in (c). Data are shown as means ± SD ($n = 11$). (e) Sheath blight disease symptoms of the indicated *arf* lines at 3 dpi with *Rhizoctonia solani* isolate AG-1-IA. Bar, 1 cm. (f) Quantitative lesion areas in the inoculated leaves in (e). The percentages of lesion area were calculated as the ratio of lesion area to the leaf area. Data are shown as means ± SD ($n = 3$). For (b, d, f), the different letters above bars indicate significant differences at $P < 0.05$ determined by one-way ANOVA followed by *post hoc* Tukey honestly significant difference analysis. ns, significant differences. Colored dots associated with the bars indicate the value of biologically independent samples.

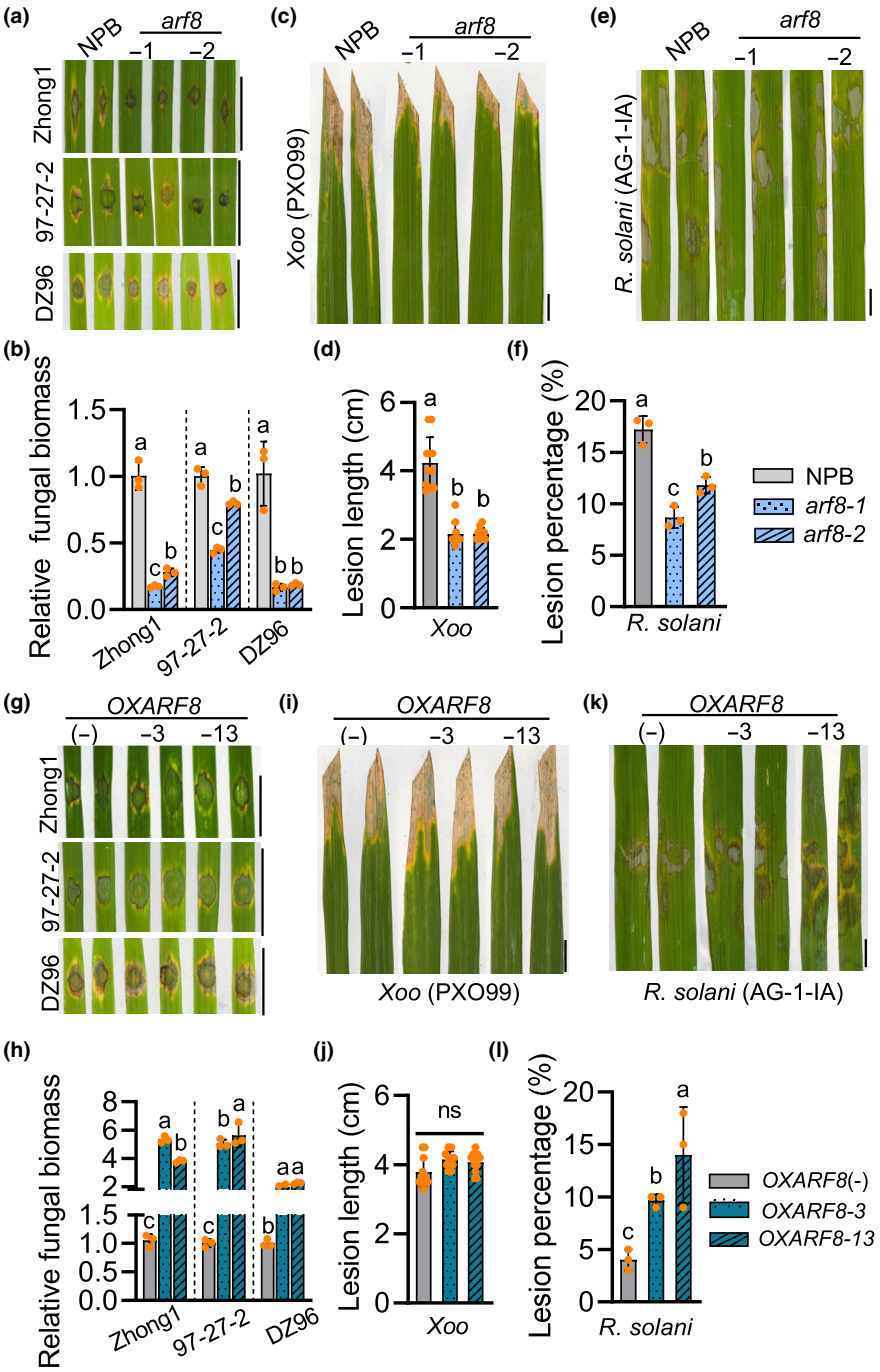

Fig. 3 Mutation of *ARF8* enhances broad-spectrum disease resistance in rice. (a) Disease symptoms of *ARF8* mutants (*arf8*) and the Nipponbare (NPB) control at 7 d post-inoculation (dpi) with *Magnaporthe oryzae* isolates Zhong1, 97-27-2 and DZ96. Bar, 1 cm. (b) Fungal biomass of *M. oryzae* isolates in the indicated lines in (a). Fungal biomass was examined by quantitative polymerase chain reaction (qPCR) and shown as the ratio of *M. oryzae MoPot2* DNA amounts against rice ubiquitin DNA amounts. Data are shown as means ± SD ($n = 3$). (c) Disease symptoms of the indicated lines at 14 dpi with *Xanthomonas oryzae* pv *oryzae* (*Xoo*) isolate PXO99. Bar, 1 cm. (d) Quantitative lesion lengths measured at 14 dpi as in (c). Data are shown as means ± SD ($n = 11$). (e) Disease symptoms at 3 dpi with *Rhizoctonia solani* isolate AG-1-IA in indicated lines. Bar, 1 cm. (f) Quantitative lesion areas after *R. solani* inoculation as in (e). The percentages of lesion area were calculated as the ratio of lesion area to the leaf area. Data are shown as means ± SD ($n = 3$). (g) Disease symptoms of *ARF8*-overexpressing lines (*OXARF8*) and the null segregant control of *OXARF8* (*OXARF8(−)*) at 7 dpi with *M. oryzae* isolates Zhong1, 97–27-2 and DZ96. Bar, 1 cm. (h) Fungal biomass of *M. oryzae* isolates in the indicated lines in (g). Fungal biomass was examined by qPCR and shown as the ratio of *M. oryzae MoPot2* DNA amounts against rice ubiquitin DNA amounts. Data are shown as means ± SD ($n = 3$). (i) Disease symptoms of the indicated lines at 14 dpi with *Xoo* isolate PXO99. Bar, 1 cm. (j) Quantitative lesion lengths measured at 14 dpi as in (i). Data are shown as means ± SD ($n = 11$). (k) Disease symptoms at 3 dpi with *R. solani* isolate AG-1-IA. Bar, 1 cm. (l) Quantitative lesion areas after *R. solani* inoculation as in (k). The percentages of lesion area were calculated as the ratio of lesion area to the leaf area. Data are shown as means ± SD ($n = 3$). In (b, d, f, h, j, l), the different letters above bars indicate significant differences at $P < 0.05$ determined by one-way ANOVA followed by *post hoc* Tukey honestly significant difference analysis, and the colored dots associated with the bars indicate the value of biologically independent samples.

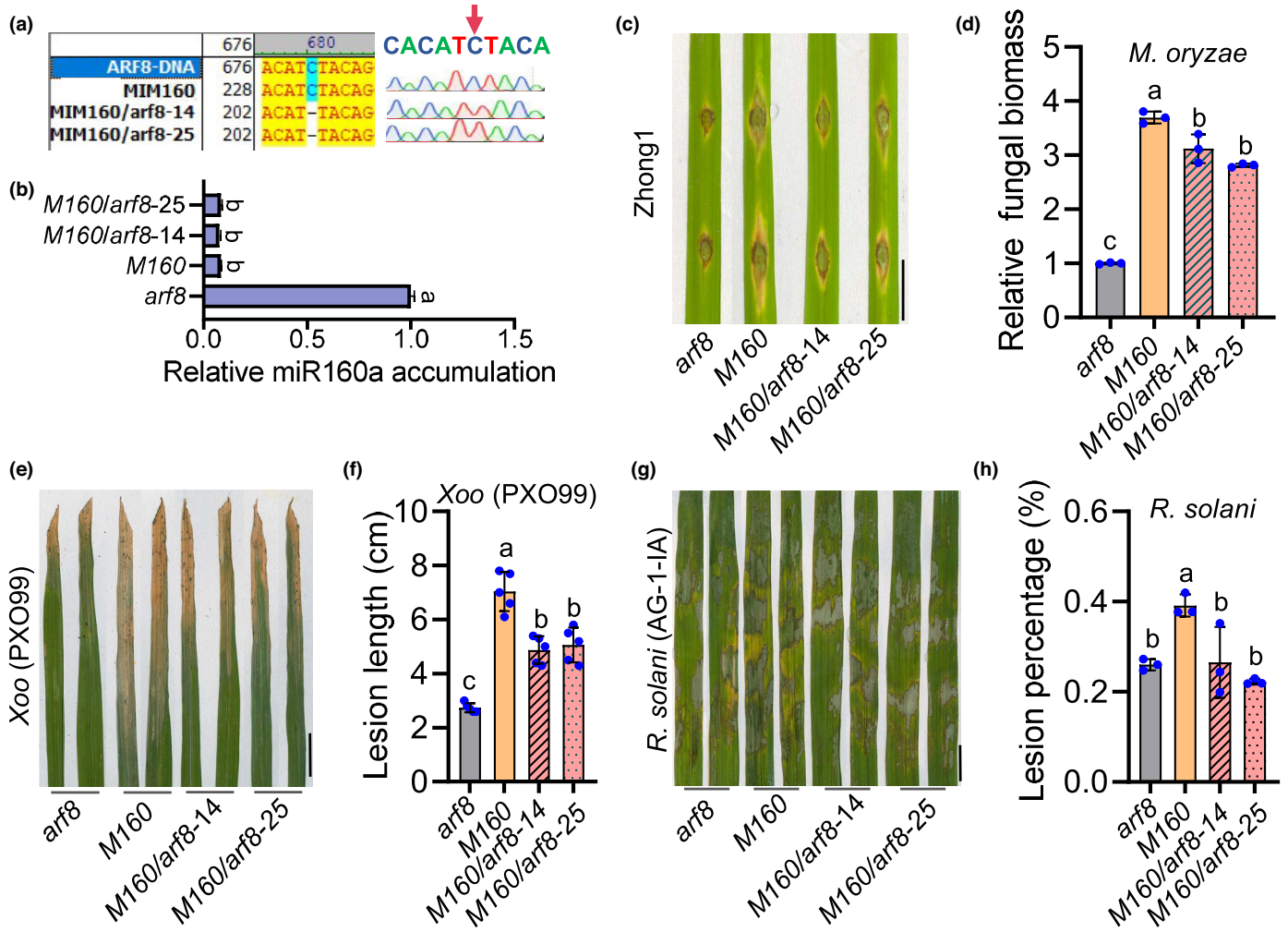

Fig. 4 Mutation of *ARF8* partially alleviates the susceptibility of *MIM160* in *MIM160/arf8* lines in rice. (a) Alignments of the genomic DNA sequences of *ARF8* in *MIM160/arf8* lines and the null segregant control (*M160*) at the mutated site. The red arrow indicates the 'C' deleted in *MIM160/arf8* lines. (b) The relative amounts of miR160a in the indicated lines. miR160a amounts were examined by stem-loop reverse-transcription quantitative polymerase chain reaction (RT-qPCR). Rice *U6* was used as an internal reference. (c) Disease symptoms of the indicated lines at 7 d post-inoculation (dpi) with *Magnaporthe oryzae* isolate Zhong1. Bar, 1 cm. (d) Fungal biomass of *M. oryzae* isolate Zhong1 in the indicated lines. Fungal biomass was examined by quantitative PCR (qPCR) and shown as the ratio of *M. oryzae MoPot2* DNA amounts against rice *ubiquitin* DNA amounts. (e) Disease symptoms of the indicated lines at 14 dpi with *Xanthomonas oryzae* pv *oryzae* (*Xoo*) isolate PXO99. Bar, 1 cm. (f) Quantitative lesion lengths measured at 14 dpi as in (e). Data are shown as means ± SD ($n = 5$). (g) Disease symptoms at 3 dpi with *Rhizoctonia solani* isolate AG-1-IA. Bar, 1 cm. (h) Quantitative lesion areas after *R. solani* inoculation as in (g). The percentages of lesion area were calculated as the ratio of lesion area to the leaf area. Data are shown as means ± SD ($n = 3$). For (b, d, f, h), data are shown as means ± SD ($n = 3$), the different letters above bars indicate significant differences at $P < 0.05$ determined by one-way ANOVA followed by *post hoc* Tukey honestly significant difference analysis, and the colored dots associated with the bars indicate the value of biologically independent samples.

To assess the role of *ARF8* in miR160a-regulated broad-spectrum resistance, we introduced the *arf8* mutation into the *MIM160* background and obtained independent homozygous *MIM160/arf8* mutants (*M160/arf8*) and a homozygous *MIM160* control expressing WT *ARF8* (*M160*; Fig. 4a,b). Upon *M. oryzae* and *Xoo* infection, the *arf8* mutation partially alleviated the susceptibility of *MIM160* in *MIM160/arf8* lines, yielding less fungal biomass and smaller disease lesions than *MIM160* but more fungal biomass and larger disease lesions than *arf8* (Fig. 4c–f). This result indicates a role for *arf8* in miR160a-mediated resistance and the existence of other miR160a target genes that participate in this process. Moreover, *MIM160/arf8* completely restored the disease phenotypes of *R. solani* (Fig. 4g,h), indicating a key role for *ARF8* in miR160a-mediated sheath blight disease resistance.

The miR160a-*ARF8* module controls rice basal defense responses

Interestingly, miR160a was significantly upregulated as early as 6–12 h post-inoculation (hpi) with the pathogens (Fig. S1b–d), indicating that miR160a is involved in early defense responses. We then explored whether *ARF8* was also responsive to PAMP-derived elicitors flg22 and chitin in NPB plants. The RT-qPCR results showed that *ARF8* expression was decreased at 3, 6, and 12 h post-treatment of flg22 or chitin (Fig. 5a), indicating that

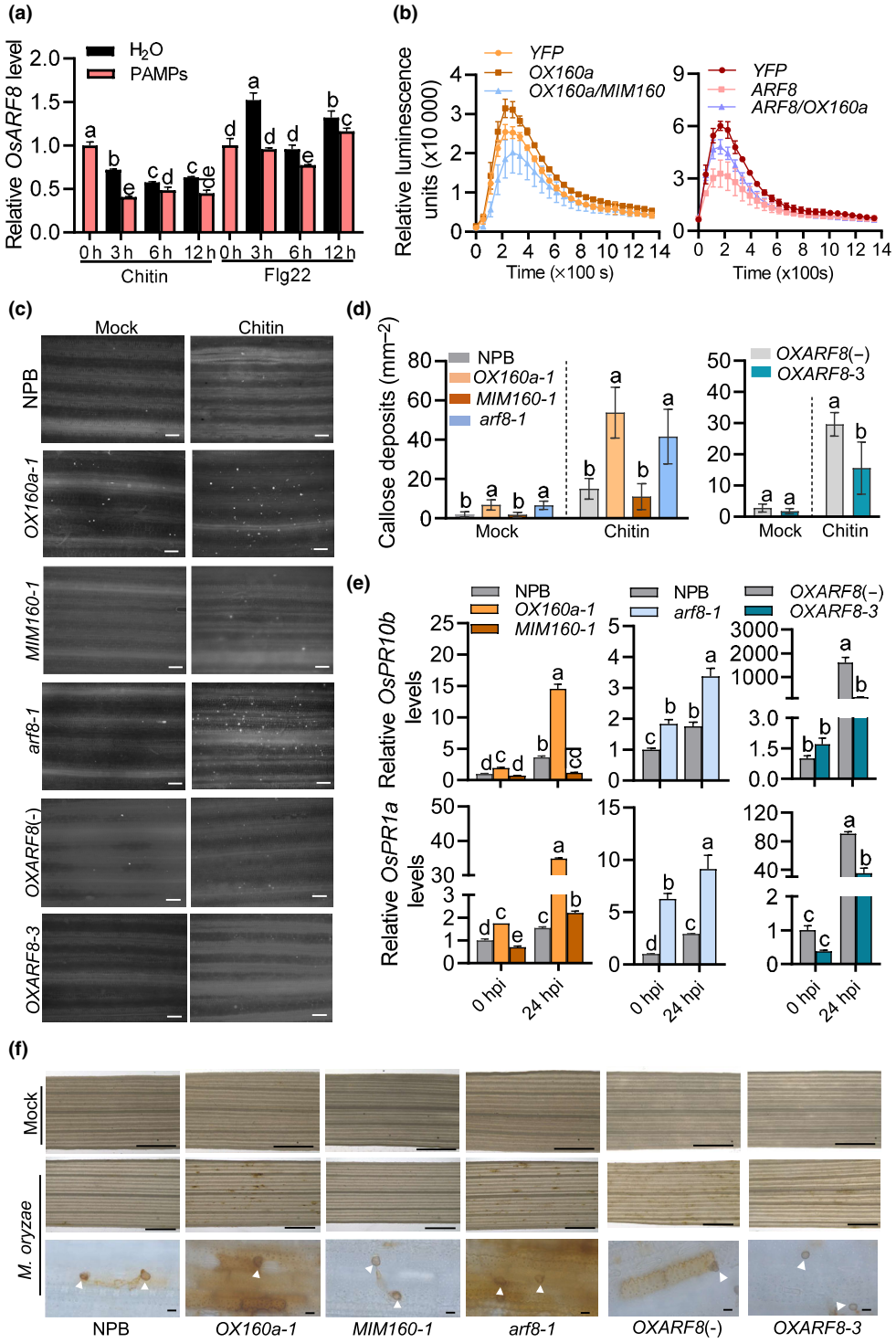

Fig. 5 miR160a-*ARF8* module regulates rice basal defense responses. (a) Reverse-transcription quantitative polymerase chain reaction (RT-qPCR) data show the expression patterns of *ARF8* following the treatment of flg22 and chitin. Data are shown as means ± SD ($n = 3$). (b) Chitin-induced reactive oxygen species (ROS) bursts in the leaves of *Nicotiana benthamiana* transiently expressing miR160a with or without *MIM160*, *Yellow Florescence Protein* (*YFP*)-*ARF8* with or without miR160a, and the *YFP* control. Data are shown as means ± SD ($n = 4$). (c) Chitin-induced callose deposition in *OX160a*, *MIM160*, *arf8*, the Nipponbare (NPB) control, *OXARF8* and the null segregant control *OXARF8*(−). Callose deposits were stained by aniline blue and appear as bright spots. Bar, 0.1 mm. (d) Quantitation of callose deposits in the indicated lines in (c). Data are shown as means ± SD ($n = 5$). (e) RT-qPCR data show the expression of *OsPR1a* and *OsPR10b* in the indicated lines at 0 and 24 h post-inoculation (hpi) with *Magnaporthe oryzae* isolate Zhong1. Data are shown as means ± SD ($n = 3$). (f) H_2O_2 accumulation in the indicated lines at 48 hpi with *M. oryzae*. 3,3′-diaminobenzidine (DAB) was used as an indicator of H_2O_2 amounts (reddish-brown). Appressoria were indicated by white triangles. Bars: (upper panels) 1 mm; (lower panels) 10 μm. For (a, d, e), the letters above bars indicate significant differences at $P < 0.05$ determined by one-way ANOVA followed by *post hoc* Tukey honestly significant difference analysis.

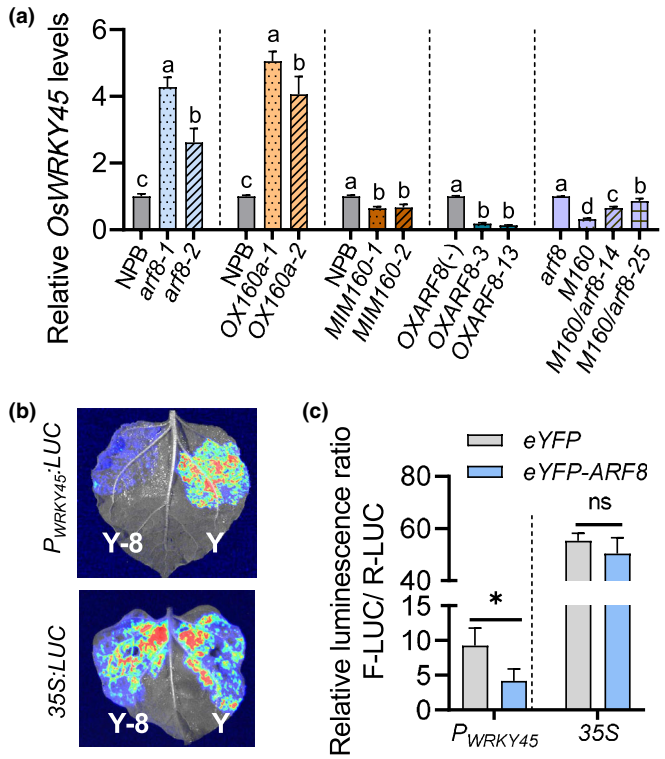

Fig. 6 ARF8 suppresses *WRKY45* expression in rice. (a) Reverse-transcription quantitative polymerase chain reaction (RT-qPCR) showing the mRNA amounts of *OsWRKY45* in *arf8*, *OX160a*, *MIM160*, the Nipponbare control, *OXARF8*, the null segregant control *OXARF8*(−), *M160/arf8* and the null segregant *M160*. (b) Firefly luciferase (*F-LUC*) expression driven by *WRKY45* promoter (P_{WRKY45}*:LUC*) or 35S promoter (*35S:LUC*). The constructs P_{WRKY45}*:LUC* or *35S:LUC* were transiently coexpressed with constructs *35S:YFP* or *35S:YFP-ARF8* in *Nicotiana benthamiana* leaves by *Agrobacterium*-mediated infiltration. The *LUC* light signals were imaged at 40 h post-infiltration. Y:YFP; Y-8:YFP-ARF8. 35S-drived *Renilla* luciferase (*R-LUC*) was coexpressed as an internal reference of transfection efficiency in individual leaves. (c) The ratio of *F-LUC*/*R-LUC* luminescence in indicated combination in (b). Firefly luminescence and *Renilla* luminescence signals were detected using the Promega GloMax® 96 Luminometer. ns, not significant. For (a) and (c), data are shown as means ± SD ($n = 3$). Different letters or asterisk above bars indicate significant differences at $P < 0.05$ determined by a one-way ANOVA followed by *post hoc* Tukey honestly significant difference analysis or by two-sided Student's *t*-test.

ARF8 is responsive to PAMPs and possibly suppresses PAMP-triggered immunity (PTI) in rice.

We then explored whether the miR160a-*ARF8* module regulated rice PTI responses. We first assessed the effects of miR160a and ARF8 on chitin-induced ROS bursts. Transient expression of miR160a in *N. benthamiana* led to enhanced ROS bursts in comparison with the control, whereas coexpressing MIM160 resulted in compromised ROS bursts (Fig. 5b), indicating that miR160a boosts chitin-triggered ROS bursts. Furthermore, overexpression of *ARF8* resulted in greatly compromised ROS bursts in comparison to the control, whereas silencing *ARF8* by expressing miR160a partly released the suppression by *ARF8* (Fig. 5b), suggesting that *ARF8* plays a negative role in ROS burst induction and that miR160a enhances ROS bursts by suppressing *ARF8*. Next, we examined chitin-induced callose deposition in the transgenic lines. Compared with the NPB control, both *OX160a* and *arf8* plants accumulated more callose following chitin treatment, whereas *MIM160* and *OXARF8* plants accumulated comparable or less callose (Fig. 5c,d), indicating that miR160a boosts, whereas *ARF8* suppresses, PAMP-induced callose deposition.

Furthermore, we also examined hydrogen peroxide (H_2O_2) accumulation by DAB staining and expression of *pathogenesis-related 1a* (*PR1a*) and *PR10b* by RT-qPCR (Midoh & Iwata, 1996; McGee *et al.*, 2001) in these lines following *M. oryzae* infection. *OX160a* and *arf8* displayed higher induction of *OsPR1a* and *OsPR10b* expression than the NPB control at 24 hpi, whereas *MIM160* and *OXARF8* showed lower induction than the controls (Fig. 5e). Similarly, *OX160a* and *arf8* mutants showed more H_2O_2 accumulation at the infection sites than did NPB, whereas *MIM160* and *OXARF8* lines displayed less H_2O_2 accumulation (Fig. 5f). These results indicate that miR160a positively regulates, whereas *ARF8* negatively regulates, pathogen-induced defense responses.

Intriguingly, *OX160a* and *arf8* exhibited constitutive enhancement of callose deposition and expression of *PR* genes without treatment, indicating a constitutive activity of defense responses. By contrast, although displaying a dwarf phenotype, *OXARF8* showed compromised or similar defense responses to the control (Fig. 5c–f). In conclusion, these results suggest that miR160a enhances, whereas *ARF8* suppresses, basal defense responses in rice.

The miR160a-*ARF8* module regulates *WRKY45* expression

To further identify the downstream signaling of *ARF8*, we conducted RNA sequencing (RNA-seq) analysis with three replications and compared the transcriptomic profiles of *arf8* and the NPB control. We surveyed 39 743 genes from the filtered data (Table S4) and identified 268 upregulated and 55 downregulated genes in *arf8* (*arf8* vs WT) using cut-off criteria of 1.5-fold change in expression ($|\log_2\text{fold change}| > 1$; $P_{adj} < 0.05$; Tables S5–S7; Methods S2). As ARF8 acts as a transcriptional repressor (Wang *et al.*, 2007), we focused on the upregulated genes. Kyoto Encyclopedia of Genes and Genomes (KEGG) pathway analysis showed that the upregulated genes are most enriched in three pathways: 'plant hormone signal transduction', 'plant–pathogen interaction' and 'MAPK signaling pathway-plant' (Fig. S5a). The three signaling pathways are extensively involved in plant immunity (Nasir *et al.*, 2018), confirming the prominent role of *ARF8* in rice immunity. Besides, gene ontology (GO) analysis revealed that the upregulated genes are significantly enriched in 'transcription factor activity, sequence-specific DNA binding', suggesting that ARF8 regulates expression of multiple transcription factors (Fig. S5b). Importantly, we found that a defense-related *WRKY* gene, *WRKY45*, was significantly upregulated in *arf8* (Table S7) (Jiang *et al.*, 2017; Viana *et al.*, 2018). We validated the expression of *WRKY45* in the transgenic lines and found that *WRKY45* mRNA concentrations were notably enhanced in two individual *arf8* mutant and *OX160a* lines (Fig. 6a), but decreased in *MIM160* and *OXARF8*. Consistently,

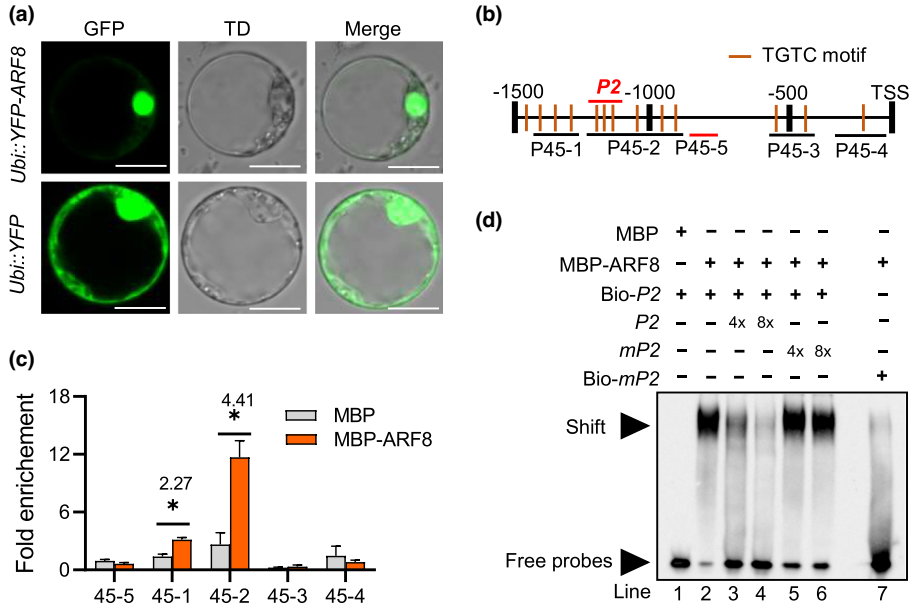

Fig. 7 ARF8 binds directly to the promoter of *WRKY45*. (a) Subcellular localization of yellow florescence protein (YFP)-fused ARF8 (YFP-ARF8) and YFP in rice protoplasts. YFP signals were observed with a fluorescence microscope at 12 h post-infiltration. Bar, 5 μm. (b) Distribution of TGTC motifs in *WRKY45* promoter. P45-1, P45-2, P45-3 and P45-4 are the fragments of the *WRKY45* promoter containing one or more TGTC motifs. P45-5 is a fragment without any TGTC motif and is used as a negative control. *P2* is a fragment containing three TGTC motifs located on P45-2. TSS, transcription start site. (c) Chromatin immunoprecipitation-quantitative polymerase chain reaction (ChIP-qPCR) data show the enrichment of the fragments (P45-1, P45-2, P45-3, P45-4, P45-5) in DNA samples pulled down by maltose-binding protein (MBP)-ARF8 or MBP. The fragment amounts were normalized to the amounts of *ubiquitin* DNA. Data are shown as means ± SD ($n = 3$). The asterisks above bars indicate significant differences at $P < 0.05$ determined by two-sided Student's *t*-test. (d) Electrophoretic mobility shift assay (EMSA) shows the direct binding of ARF8 to the *WRKY45* promoter. Bio-*P2* is a 50-bp-long biotin-labeled probe containing three TGTC motifs from P45-2. *mP2* is a mutation of *P2* in which the three TGTC motifs were mutated into TTTT. The unlabeled *P2* and *mP2* were used as competitors in four- and eight-fold excess to the biotin-labeled probes. +, addition; –, means no addition. These experiments were repeated at least twice and produced similar results.

WRKY45 mRNA concentrations were partially restored in *MIM160/arf8* in comparison to that of *arf8* (Fig. 6a). These data indicate that miR160a enhances *WKRY45* expression by suppressing *ARF8*.

The ARFs likely act as transcription factors to regulate downstream genes. We tested whether ARF8 directly represses the promoter activity of *WRKY45* in *N. benthamiana* using a dual-luciferase reporter assay (Fig. 6b,c). We coexpressed yellow fluorescent protein (YFP)-fused *ARF8* or a YFP control with the firefly luciferase reporter driven by the *WRKY45* promoters or by 35S promoter. A Renilla luciferase driven by *35S* promoter was coexpressed as an internal reference to normalize the transformation efficiency. Compared with the *YFP* control, *YFP-ARF8* almost completely blocked luciferase expression from the *WRKY45* promoter, but had only mild effects on the 35S promoter (Fig. 6b,c), suggesting that that ARF8 suppressed the activity of the *WRKY45* promoter.

ARF8 binds directly to the *WRKY45* promoter

We next explored whether ARF8 binds directly to the promoter of *WRKY45*. We first analyzed the subcellular localization of the YFP-ARF8 protein and found that it was specifically localized in the nucleus. By contrast, the YFP control was localized in both cytoplasm and the nucleus (Fig. 7a). We then used a yeast one-hybrid system to test the binding of ARF8 to the *WRKY45* promoter (Methods S3). However, we did not observe yeast growth, possibly because of the strong repression by ARF8 on the *WRKY45* promoter and hence on yeast growth (Fig. S6). Therefore, we conducted *in vitro* ChIP-qPCR and EMSA to test the binding of ARF8 to the *WRKY45* promoter. For the *WRKY45* promoter (P45), we selected a 1.5 kb DNA sequence before the transcription start site of *WRKY45*. ARF proteins are known to bind the TGTC motif (Shen *et al.*, 2010; Zhang *et al.*, 2015; Qin *et al.*, 2020). We analyzed the sequence of *WRKY45* promoter and found 13 putative TGTC motifs. We divided the promoter into five fragments according to the locations of the TGTC motifs: P45-1 (−1446 to −1208 with three TGTC motifs), P45-2 (−1154 to −842 with six motifs), P45-3 (−726 to −421 with two motifs), P45-4 (−180 to −53 with one motif), and P45-5 (−854 to −737 without TGTC motifs) which was used as a negative control (Fig. 7b). We conducted expression of the ARF8 protein tagged with MBP in *E. coli* (Fig. S7; Methods S4). The ChIP-qPCR data showed that P45-1 and, in particular, P45-2 were significantly enriched in the DNA pulled down by MBP-ARF8 up to 4.41-fold compared with the MBP control, whereas P45-3 and P45-4 were not (Fig. 7c), implying that ARF8 preferentially binds TGTC motifs in P45-2.

To further confirm the binding of ARF8 to the TGTC motifs in P45-2, we amplified a 50-bp sequence of the P45-2 fragment containing three TGTC motifs (*P2*) and a mutated *P2* fragment, in which the TGTC core sequences were mutated into TTTT

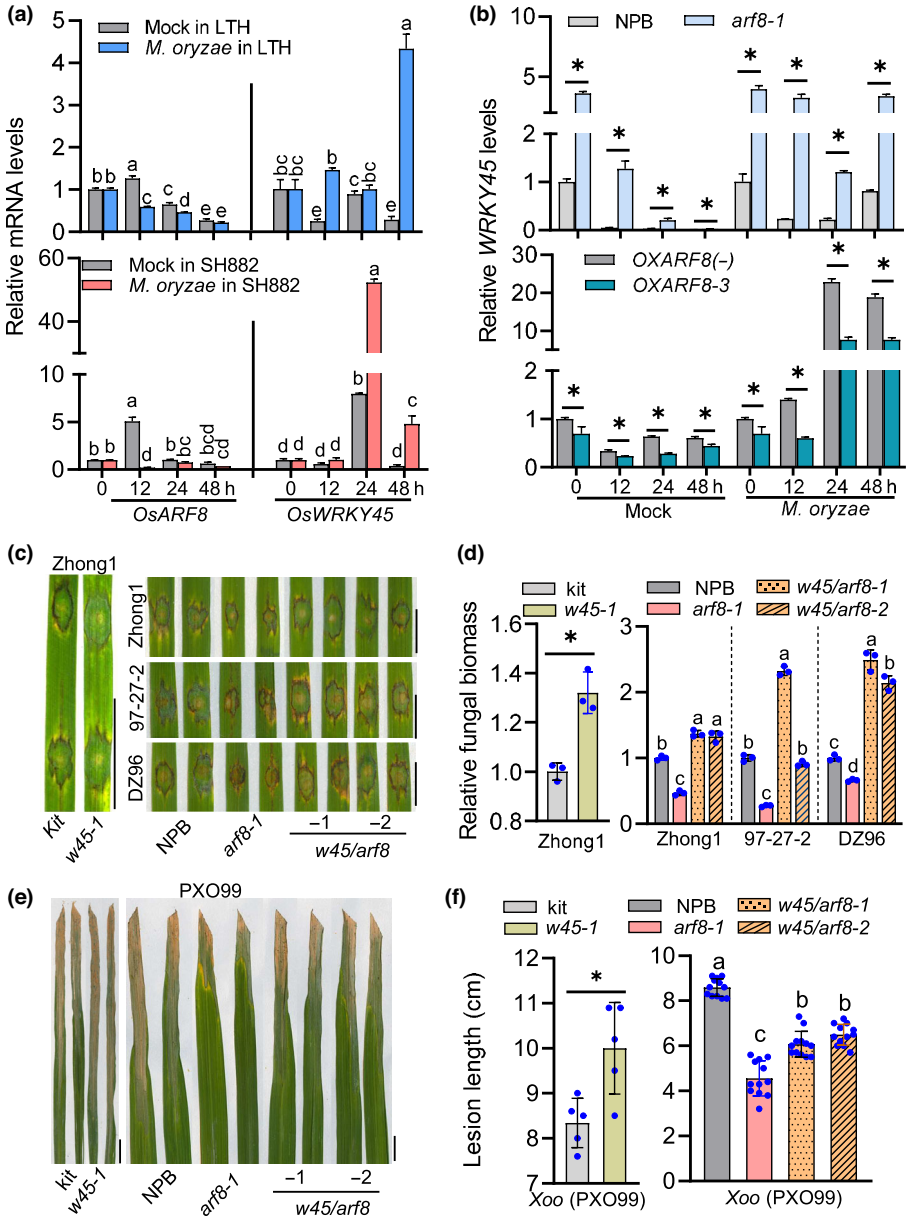

Fig. 8 ARF8 regulates broad-spectrum disease resistance via *WRKY45* in rice. (a) Reverse-transcription quantitative polymerase chain reaction (RT-qPCR) data show the expression patterns of *ARF8* and *WRKY45* at 0, 12, 24 and 48 h post-inoculation (hpi) of *Magnaporthe oryzae* isolate Zhong1 or H_2O (mock) in susceptible cv Lijiang xin Tuan Heigu (LTH) and resistant cv Shuhui882 (SH882). (b) RT-qPCR data show the expression patterns of *WRKY45* at 0, 12, 24 and 48 hpi of Zhong1 or H_2O (mock) in *arf8* and the Nipponbare (NPB) control, and in *OXARF8* and the null segregant control *OXARF8*(−). (c) Disease symptoms of *wrky45* (*w45*), the wild-type Kitaake control (*Kit*), *arf8-1*, *w45/arf8* and NPB control at 7 d post-inoculation (dpi) with *M. oryzae* isolates. Bar, 1 cm. (d) The fungal biomass of indicated *M. oryzae* isolates in the indicated lines in (c). Fungal biomass was examined by quantitative PCR (qPCR) and presented as the ratio of *M. oryzae MoPot2* DNA amounts against rice *ubiquitin* DNA amounts. (e) Disease symptoms of the indicated lines at 14 dpi with *Xanthomonas oryzae* pv *oryzae* (*Xoo*) isolate PXO99. Bar, 1 cm. (f) Quantitative lesion lengths measured at 14 dpi as in (e). For (a), (b) and (d), data are shown as means ± SD ($n = 3$). For (f), data are shown as means ± SD ($n = 5$ or 12). Different letters or the asterisks above bars indicate significant differences at $P < 0.05$ determined by a one-way ANOVA followed by *post hoc* Tukey honestly significant difference analysis or by two-sided Student's *t*-test, and the colored dots associated with the bars indicate the value of biologically independent samples.

(*mP2*). We tagged the fragments with biotin at both the 5′- and 3′-termini (Bio-*P2* and Bio-*mP2*). The EMSA results showed that MBP-ARF8 failed to bind to Bio-*mP2* (Fig. 7d, Lane 7). By contrast, MBP-ARF8 bound to Bio-*P2*, causing a shift up (Fig. 7d, Lane 2), which was greatly reduced by the unlabeled *P2* competitor (Fig. 7d, Lane 3–4), but not by the unlabeled *mP2* competitor (Fig. 7d, Lane 5–6). These results indicate that ARF8 binds directly to the P45-2 region in the *WRKY45* promoter, and that the TGTC motifs in P45-2 are required for the binding.

ARF8 regulates disease resistance against *M. oryzae* and *Xoo* via *WRKY45* in rice

Notably, *WRKY45* positively regulates disease resistance to *M. oryzae* (Shimono *et al.*, 2007; Inoue *et al.*, 2013; J. Wang *et al.*, 2018). We first explored whether *ARF8* and *WRKY45* were responsive to *M. oryzae*. We examined the expression patterns of *ARF8* and *WRKY45* in a susceptible cv LTH and a resistant cv SH882 that is widely exploited in southwest China. *ARF8* expression levels were repressed, whereas *WRKY45* levels were enhanced upon *M. oryzae* infection in both cultivars (Fig. 8a), indicating that the ARF8-*WRKY45* module is responsive to *M. oryzae*, which promotes *WRKY45* expression via repressing *ARF8*.

To further explore whether ARF8 regulates the expression of *WRKY45* during pathogen infection, we examined the expression of *WRKY45* in *OXARF8* and *arf8* with or without *M. oryzae* infection. As shown in Fig. 8b, although the expression levels of *WRKY45* were enhanced upon *M. oryzae* inoculation, they were enhanced to much higher levels in *arf8* than in the NPB control, but were suppressed in *OXARF8* compared with those in the negative control. These results confirm that ARF8 suppresses *WRKY45* induction during pathogen infection.

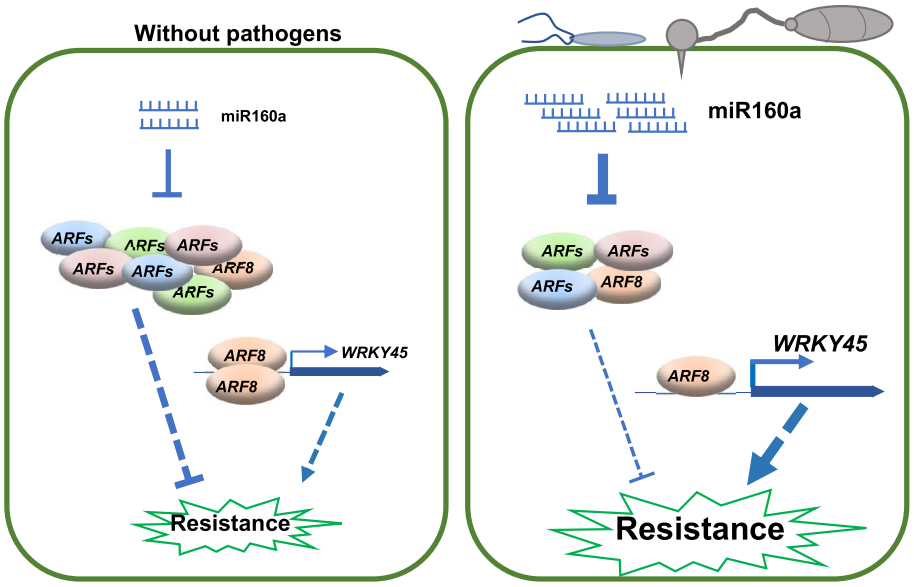

Fig. 9 A work model depicting the underlying mechanism by which miR160a regulates rice broad-spectrum disease resistance. Without pathogen infection, miR160a controls disease resistance at a low level to maintain rice normal growth by suppressing the expression of *ARFs*, which play different roles in rice resistance against different pathogens. miR160a suppresses the expression of *ARF8*, which negatively regulates broad-spectrum disease resistance and suppresses the transcription of *WRKY45*, a key regulator of disease resistance in rice. Upon pathogen infection, the increased accumulation of miR160a leads to significant reduction of *ARFs*. The reduction of ARF8 releases the suppression on *WRKY45* and thus results in enhanced disease resistance. In summary, the increased miR160a enhances broad-spectrum resistance against the causative agents of the most serious rice diseases by repressing the expression of *ARFs*. The solid arrows indicate direct enhancement, and the dashed arrows indicate indirect enhancement. The solid blunt-ended arrows indicate direct suppression, and the dashed blunt-ended arrows indicate indirect suppression. The thick arrows indicate enhanced function, and the thin arrows indicate depressed function.

WRKY45 has been identified as a positive regulator of rice blast disease resistance (Shimono *et al.*, 2007, 2012). We generated an *WRKY45* mutant line which carried a guanine (G) insertion creating mutated protein (*w45-1*; Fig. S8a). *w45-1* displayed compromised resistance against *M. oryzae* and *Xoo* compared with the Kitaake control (*Kit*; Fig. 8c–f). To further determine whether *WRKY45* contributes to the resistance mediated by the miR160a-*ARF8* module, we mutated *WRKY45* in the *arf8-1* background via CRISPR/Cas9 technology and obtained two independent *wrky45/arf8* homozygous mutants. *wrky45/arf8-1* carried a two-base deletion, creating a mutated protein, and *wrky45/arf8-2* carried a one-base deletion, creating a stop codon leading to truncated protein accompanied by decreased *WRKY45* transcript abundances (Fig. S8b,c). The double mutant lines abolished blast disease resistance conferred by *arf8*, displaying larger disease lesions and more fungal biomass than *arf8* (Fig. 8c,d), and compromised leaf blight resistance, showing longer disease lesions than *arf8* (Fig. 8e,f), indicating a crucial role for *WRKY45* in *arf8*-regulated resistance against *M. oryzae* and *Xoo*.

By contrast, the *w45-1* single mutant displayed enhanced resistance against *R. solani*, indicating a negative role for *WRKY45* in rice sheath blight disease resistance. However, *wrky45/arf8* displayed a similar degree of resistance as *arf8* (Fig. S8d,e). These results indicate that the *ARF8-WRKY45* module plays a minor role in the regulation of sheath blight disease resistance and that *WRKY45* is probably involved in an miR160a-*ARF8*-independent pathway.

Discussion

Here we summarize our results with a working model: miR160a enhances broad-spectrum disease resistance by suppressing expression of a group of *ARF* genes playing different roles in the regulation of disease resistance in rice (Fig. 9). In the absence of pathogen infection, miR160a accumulates at a certain level to boost rice immune responses by suppressing the expression of *ARFs*, which play different roles in disease resistance. In the presence of pathogens, the accumulation of miR160a is triggered, resulting in enhanced resistance to pathogens with reduced levels of *ARFs*. Among these ARFs, ARF8 acts as a negative regulator of broad-spectrum disease resistance by directly binding the promoter and suppresses the transcription of *WRKY45*, which encodes a key regulator of disease resistance. As a result, miR160a partially regulates rice broad-spectrum resistance by suppressing *ARF8* to enhance *WRKY45* expression.

Breeding resistance cultivars is the most effective and environmentally friendly strategy to guarantee food supply and food security worldwide. The utilization of resistance (*R*) genes in crops is the most popular and effective method to enhance resistance against specific pathogens. However, *R* gene-conferred resistance is usually limited to a specific pathogen race and easily breaks down as a result of rapid evolution of the cognate pathogen-derived avirulent genes. Therefore, genes that confer durable, broad-spectrum resistance to crops are desired by breeders. Currently, only a very limited number of genes are known to confer disease resistance against multiple species of pathogens.

For example, *RESISTANCE TO POWDERY MILDEW8.1* (*RPW8.1*) encodes an atypical R protein that confers resistance to both powdery mildew and bacterial pathogen *Pseudomonas syringae DC3000* (Xiao *et al.*, 2001; Zhao *et al.*, 2021). Ectopic expression of *RPW8.1* in rice promotes resistance against both *M. oryzae* and *Xoo*, implying broad-spectrum resistance in rice (Y. Li *et al.*, 2018). *OsMESL* encodes a methyl esterase-like protein that confers broad-spectrum resistance to *Xoo* and *R. solani* in rice by interacting with OsTrxm, a ROS-scavenging regulator involved in downstream jasmonic acid signaling (Hu *et al.*, 2021). In this study, we identified miR160a and ARF8 as broad-spectrum resistance regulators in response to multiple pathogens, including *M. oryzae*, *Xoo* and *R. solani* (Figs 1–3). Our results provide novel candidate genes for crop breeding to improve broad-spectrum resistance against pathogens.

Several studies revealed that the miR160a-*ARFs* module is involved in the regulation of plant biotic and abiotic stress responses. In *Arabidopsis*, miR160a overexpression significantly suppresses *AtARF16* and *AtARF17* expression and enhances callose deposition induced by flg22 as well as the *hrcC*$^{-}$ mutant bacterium that is deficient in type III secretion system, suggesting that miR160a probably regulates PTI via *AtARF16* and *AtARF17* in Arabidopsis (Li *et al.*, 2010). In potato, miR160a targets *StARF10* to regulate the expression of *StGH3.6*, a mediator of the cross-talk between salicylic acid and auxin, thus playing a crucial role in local defense and systemic aquired resistance responses during *Phytophthora infestans* infection (Natarajan *et al.*, 2018). Besides, miR160a positively regulates drought tolerance by promoting adventitious root development via *MdARF17* in apples (Shen *et al.*, 2022). These observations indicate that the miR160a-*ARFs* module is conserved among plants and functions widely in response to biotic and abiotic stresses. In this study, we demonstrate that miR160a coordinates four *ARFs* playing different roles in disease resistance in rice (Figs 2, 3). *ARF8* negatively regulates broad-spectrum disease resistance against *M. oryzae*, *Xoo* and *R. solani* in rice because *arf8* enhances resistance to all three pathogens (Fig. 3). Similarly, mutations of *ARF22* or *ARF18* enhance resistance against *M. oryzae* and *Xoo* (Fig. 2). However, mutations of *ARF22* have little effects on resistance against *R. solani*, and mutations of *ARF18* enhance susceptibility to *R. solani* (Fig. 2). By contrast, mutations of *ARF10* enhances the susceptibility to *M. oryzae* and *Xoo*, but has no significant effects on resistance against *R. solani* (Fig. 2). How miR160a coordinates these *ARFs* to improve broad-spectrum disease resistance in rice is a complex process.

In rice, 25 *ARF* members have been identified (Wang *et al.*, 2007). Another miRNA, miR167d, also targets *ARFs*, including *ARF6, ARF12, ARF17* and *ARF25*, which are also responsive to *M. oryzae* (Zhao *et al.*, 2020). However, the roles of these *ARFs* in disease resistance in rice are unclear. It is unknown whether these miR167d-targeted *ARFs* and miR160a-targeted *ARFs* collaborate in the regulation of broad-spectrum disease resistance in rice.

In this study, we demonstrate that *ARF8* binds directly to the *WRKY45* promoter and suppresses its expression (Figs 6, 7). Mutations of *ARF8* lead to enhanced disease resistance, whereas overexpression of *ARF8* or mutations of *WRKY45* result in compromised resistance (Fig. 8). Consistently, mutations of *WRKY45* in the *arf8* background null the resistance against *M. oryzae* and *Xoo* conferred by *arf8*, confirming the role of *WRKY45* downstream of the miR160a-*ARF8* module (Fig. 8). Conversely, *WRKY45* negatively regulates resistance against *R. solani*, and *wrky45*/*arf8* double mutant lines display a similar degree of resistance to *arf8* (Fig. S8), indicating that *WRKY45* is involved in another signaling pathway independent of *arf8*, and the existence of a complex regulatory network controlling rice sheath blight disease resistance. It is possible that the miR160a-*ARF8* module regulates rice sheath blight resistance through coordination of a *WRKY45*-regualted signaling pathway and other pathways that possibly play a dominant role in sheath blight resistance.

Breeders try to characterize and use genes to improve broad-spectrum resistance in crops without yield penalty. Specifically, ARF proteins act as key components in the auxin signaling pathway involved in the regulation of seed development (Cao *et al.*, 2020). In rice, many *ARF* members play important roles in controlling grain size. For example, *ARF4* knockout leads to a larger grain with increased grain length and grain width (Hu *et al.*, 2018), Loss of function of *ARF6* results in increased grain length (Qiao *et al.*, 2021). By contrast, mutation of *OsARF11* leads to smaller seeds with decreased grain length and grain width (Sims *et al.*, 2021). Furthermore, overexpression of miR160a-insensitive *OsARF18* causes decreased grain width without affecting grain length (Huang *et al.*, 2016), indicating that miR160a may also target other *ARFs* to regulate grain size. Further research is needed to reveal the roles of miR160a and its target genes in the regulation of grain development and grain size.

Acknowledgements

We thank Prof. Xue-wei Chen (State Key Laboratory of Crop Gene Exploration and Utilization in Southwest China, Sichuan Agricultural University) for providing seeds of *wrky45*, and Prof. Yu-Ping Wang (State Key Laboratory of Crop Gene Exploration and Utilization in Southwest China, Sichuan Agricultural University) for providing seeds of SH882. This work was supported by the National Natural Science Foundation of China (nos. 32172417, U19A2033 and 31430072), the Department of Science and Technology of Sichuan Province (2022JDTD0023 and 2021YJ0304) and the Open Research Fund of State Key Laboratory of Hybrid Rice (Hunan Hybrid Rice Research Center, 2021KF07).

Author contributions

YL and W-MW conceived the experiment, and carried it out together with QF, HW, X-MY, Z-WH, X-HZ, LX, X-YX, X-RH, YZ and G-BL; J-HZ, X-HH, J-WZ, Z-XZ, JF and Y-YH analyzed the data; Y-PJ, S-XZ and MP carried out the field trial; and YL and W-MW wrote the paper.

ORCID

Jing Fan https://orcid.org/0000-0002-6747-4302
Qin Feng https://orcid.org/0000-0002-9274-8010

Xiao-Rong He https://orcid.org/0000-0002-8438-8414
Xiao-Hong Hu https://orcid.org/0000-0003-3104-0876
Zhang-Wei Hu https://orcid.org/0000-0001-9248-3078
Yan-Yan Huang https://orcid.org/0000-0001-7688-0997
Guo-Bang Li https://orcid.org/0000-0001-5333-9321
Yan Li https://orcid.org/0000-0002-6443-9245
He Wang https://orcid.org/0000-0001-9654-6283
Wen-Ming Wang https://orcid.org/0000-0002-6652-5964
Ling Xiang https://orcid.org/0000-0002-6255-4047
Xiao-Yu Xiong https://orcid.org/0000-0001-8099-2350
Xue-Mei Yang https://orcid.org/0000-0002-2546-5723
Ji-Wei Zhang https://orcid.org/0000-0001-7402-4089
Jing-Hao Zhao https://orcid.org/0000-0002-1347-3056
Zhi-Xue Zhao https://orcid.org/0000-0002-3450-8422
Shi-Xin Zhou https://orcid.org/0000-0001-8055-3569
Xin-Hui Zhou https://orcid.org/0000-0003-2459-9911
Yong Zhu https://orcid.org/0000-0001-8311-1336

Data availability

The data that support the findings of this study are available from the corresponding author upon reasonable request.

References

Campo S, Peris-Peris C, Siré C, Moreno AB, Donaire L, Zytnicki M, Notredame C, Llave C, San Segundo B. 2013. Identification of a novel microRNA (miRNA) from rice that targets an alternatively spliced transcript of the *Nramp6* (*Natural resistance-associated macrophage protein 6*) gene involved in pathogen resistance. *New Phytolosist* **199**: 212–227.

Campo S, Sánchez-Sanuy F, Camargo-Ramírez R, Gómez-Ariza J, Baldrich P, Campos-Soriano L, Soto-Suárez M, San Segundo B. 2021. A novel transposable element-derived microRNA participates in plant immunity to rice blast disease. *Plant Biotechnology Journal* **19**: 1798–1811.

Cao J, Li G, Qu D, Li X, Wang Y. 2020. Into the seed: auxin controls seed development and grain yield. *International Journal of Molecular Sciences* **21**: 1662.

Chandran V, Wang H, Gao F, Cao XL, Chen YP, Li GB, Zhu Y, Yang XM, Zhang LL, Zhao ZX *et al.* 2018. miR396-OsGRFs module balances growth and rice blast disease-resistance. *Frontiers in Plant Science* **9**: 1999.

Chen JF, Zhao ZX, Li Y, Li TT, Zhu Y, Yang XM, Zhou SX, Wang H, Zhao JQ, Pu M *et al.* 2021. Fine-tuning roles of Osa-miR159a in rice immunity against *Magnaporthe oryzae* and development. *Rice* **14**: 26.

Elert E. 2014. Rice by the numbers: a good grain. *Nature* **514**: S50–S51.

Fabian MR, Sonenberg N, Filipowicz W. 2010. Regulation of mRNA translation and stability by microRNAs. *Annual Review of Biochemistry* **79**: 351–379.

Gnanamanickam SS, Priyadarisini VB, Narayanan NN, Vasudevan P, Kavitha S. 1999. An overview of bacterial blight disease of rice and strategies for its management. *Current Science* **77**: 1435–1444.

He F, Chen S, Ning YS, Wang GL. 2016. Rice (*Oryza sativa*) protoplast isolation and its application for transient expression analysis. *Current Protocols in Plant Biology* **1**: 373–383.

Hu B, Zhou Y, Zhou Z, Sun B, Zhou F, Yin C, Ma W, Chen H, Lin Y. 2021. Repressed *OsMESL* expression triggers reactive oxygen species-mediated broad-spectrum disease resistance in rice. *Plant Biotechnol Journal* **19**: 1511–1522.

Hu Z, Lu SJ, Wang MJ, He H, Sun L, Wang H, Liu XH, Jiang L, Sun JL, Xin X *et al.* 2018. A novel QTL q*TGW3* encodes the GSK3/SHAGGY-like kinase OsGSK5/OsSK41 that interacts with OsARF4 to negatively regulate grain size and weight in rice. *Molecular Plant* **11**: 736–749.

Huang J, Li Z, Zhao D. 2016. Deregulation of the OsmiR160 target gene *OsARF18* causes growth and developmental defects with an alteration of auxin signaling in rice. *Scientific Reports* **6**: 29938.

Inoue H, Hayashi N, Matsushita A, Xinqiong L, Nakayama A, Sugano S, Jiang CJ, Takatsuji H. 2013. Blast resistance of CC-NB-LRR protein Pb1 is mediated by WRKY45 through protein-protein interaction. *Proceedings of the National Academy of Science, USA* **110**: 9577–9582.

Jia Y, Li C, Li Q, Liu P, Liu D, Liu Z, Wang Y, Jiang G, Zhai W. 2020. Characteristic dissection of *Xanthomonas oryzae* pv *oryzae* responsive microRNAs in rice. *International Journal of Molecular Sciences* **21**: 785.

Jiang J, Ma S, Ye N, Jiang M, Cao J, Zhang J. 2017. WRKY transcription factors in plant responses to stresses. *Journal of Integrative Plant Biology* **59**: 86–101.

John Lilly J, Subramanian B. 2019. Gene network mediated by *WRKY13* to regulate resistance against sheath infecting fungi in rice (*Oryza sativa* L.). *Plant Science* **280**: 269–282.

Kim S, Kim CY, Park SY, Kim KT, Jeon J, Chung H, Choi G, Kwon S, Choi J, Jeon J *et al.* 2020. Two nuclear effectors of the rice blast fungus modulate host immunity via transcriptional reprogramming. *Nature Communications* **11**: 5845.

Lee FN, Rush MC. 1983. Rice sheath blight: a major rice disease. *Plant Disease Reporter* **67**: 829–832.

Li W, Jia Y, Liu F, Wang F, Fan F, Wang J, Zhu J, Xu Y, Zhong W, Yang J. 2019. Integration analysis of small RNA and degradome sequencing reveals microRNAs responsive to *Dickeya zeae* in resistant rice. *International Journal of Molecular Sciences* **20**: 222.

Li W, Zhu Z, Chern M, Yin J, Yang C, Ran L, Cheng M, He M, Wang K, Wang J *et al.* 2017. A natural allele of a transcription factor in rice confers broad-spectrum blast resistance. *Cell* **170**: 114–126.

Li WQ, Jia YL, Liu FQ, Wang FQ, Fan FJ, Wang J, Zhu JY, Xu Y, Zhong WG, Yang J. 2018. Genome-wide identification and characterization of long non-coding RNAs responsive to *Dickeya zeae* in rice. *RSC Advances* **8**: 34408–34417.

Li XP, Ma XC, Wang H, Zhu Y, Liu XX, Li TT, Zheng YP, Zhao JQ, Zhang JW, Huang YY *et al.* 2020. Osa-miR162a fine-tunes rice resistance to *Magnaporthe oryzae* and yield. *Rice* **13**: 38.

Li Y, Cao XL, Zhu Y, Yang XM, Zhang KN, Xiao ZY, Wang H, Zhao JH, Zhang LL, Li GB *et al.* 2019. Osa-miR398b boosts H_2O_2 production and rice blast disease-resistance via multiple superoxide dismutases. *New Phytolosist* **222**: 1507–1522.

Li Y, Li TT, He XR, Zhu Y, Feng Q, Yang XM, Zhou XH, Li GB, Ji YP, Zhao JH *et al.* 2022a. Blocking Osa-miR1871 enhances rice resistance against *Magnaporthe oryzae* and yield. *Plant Biotechnol Journal* **20**: 646–659.

Li Y, Lu YG, Shi Y, Wu L, Xu YJ, Huang F, Guo XY, Zhang Y, Fan J, Zhao JQ *et al.* 2014. Multiple rice microRNAs are involved in immunity against the blast fungus *Magnaporthe oryzae*. *Plant Physiology* **164**: 1077–1092.

Li Y, Tong Y, He X, Zhu Y, Li T, Lin X, Mao W, Ghulam Nabi Gishkori Z, Zhao Z, Zhang J *et al.* 2022b. The rice miR171b–SCL6-IIs module controls blast resistance, grain yield, and flowering. *The Crop Journal* **10**: 117–127.

Li Y, Wang LF, Bhutto SH, He XR, Yang XM, Zhou XH, Lin XY, Rajput AA, Li GB, Zhao JH *et al.* 2021a. Blocking miR530 improves rice resistance, yield, and maturity. *Frontiers in Plant Science* **12**: 729560.

Li Y, Zhang Q, Zhang J, Wu L, Qi Y, Zhou JM. 2010. Identification of microRNAs involved in pathogen-associated molecular pattern-triggered plant innate immunity. *Plant Physiology* **152**: 2222–2231.

Li Y, Zhang Y, Wang QX, Wang TT, Cao XL, Zhao ZX, Zhao SL, Xu YJ, Xiao ZY, Li JL *et al.* 2018. *RESISTANCE TO POWDERY MILDEW8.1* boosts pattern-triggered immunity against multiple pathogens in Arabidopsis and rice. *Plant Biotechnol Journal* **16**: 428–441.

Li Y, Zhao SL, Li JL, Hu XH, Wang H, Cao XL, Xu YJ, Zhao ZX, Xiao ZY, Yang N *et al.* 2017. Osa-miR169 negatively regulates rice immunity against the blast fungus *Magnaporthe oryzae*. *Frontiers in Plant Science* **8**: 2.

Li Y, Zheng YP, Zhou XH, Yang XM, He XR, Feng Q, Zhu Y, Li GB, Wang H, Zhao JH *et al.* 2021b. Rice miR1432 fine-tunes the balance of yield and blast disease resistance via different modules. *Rice* **14**: 87.

Lian S, Cho WK, Kim SM, Choi H, Kim KH. 2016. Time-course small RNA profiling reveals rice miRNAs and their target genes in response to rice stripe virus infection. *PLoS ONE* **11**: e0162319.

Lin R, He L, He J, Qin P, Wang Y, Deng Q, Yang X, Li S, Wang S, Wang W *et al.* 2016. Comprehensive analysis of microRNA-Seq and target mRNAs of rice sheath blight pathogen provides new insights into pathogenic regulatory mechanisms. *DNA Research* **23**: 415–425.

Liu M, Shi Z, Zhang X, Wang M, Zhang L, Zheng K, Liu J, Hu X, Di C, Qian Q *et al.* 2019. Inducible overexpression of *Ideal Plant Architecture1* improves both yield and disease resistance in rice. *Nature Plants* **5**: 389–400.

Liu Q, Li X, Yan S, Yu T, Yang J, Dong J, Zhang S, Zhao J, Yang T, Mao X *et al.* 2018. *OsWRKY67* positively regulates blast and bacteria blight resistance by direct activation of *PR* genes in rice. *BMC Plant Biology* **18**: 257.

Lu J, Yang X, Chen J, Li T, Hu Z, Xie Y, Li J, Zhao J, Pu M, Feng H *et al.* 2021. Osa-miR439 negatively regulates rice immunity against *Magnaporthe oryzae*. *Rice Science* **28**: 156–165.

McGee JD, Hamer JE, Hodges TK. 2001. Characterization of a *PR*-10 *pathogenesis*-related gene family induced in rice during infection with *Magnaporthe grisea*. *Molecular Plant–Microbe Interactions* **14**: 877–886.

Midoh N, Iwata M. 1996. Cloning and characterization of a probenazole-inducible gene for an intracellular *pathogenesis*-related protein in rice. *Plant Cell Physiology* **37**: 9–18.

Nasir F, Tian L, Chang C, Li X, Gao Y, Tran LP, Tian C. 2018. Current understanding of pattern-triggered immunity and hormone-mediated defense in rice (*Oryza sativa*) in response to *Magnaporthe oryzae* infection. *Seminars in Cell and Developmental Biology* **83**: 95–105.

Natarajan B, Kalsi HS, Godbole P, Malankar N, Thiagarayaselvam A, Siddappa S, Thulasiram HV, Chakrabarti SK, Banerjee AK. 2018. MiRNA160 is associated with local defense and systemic acquired resistance against *Phytophthora infestans* infection in potato. *Journal of Experimental Botany* **69**: 2023–2036.

Park CH, Chen S, Shirsekar G, Zhou B, Khang CH, Songkumarn P, Afzal AJ, Ning Y, Wang R, Bellizzi M *et al.* 2012. The *Magnaporthe oryzae* effector AvrPiz-t targets the RING E3 ubiquitin ligase APIP6 to suppress pathogen-associated molecular pattern-triggered immunity in rice. *Plant Cell* **24**: 4748–4762.

Qiao J, Jiang H, Lin Y, Shang L, Wang M, Li D, Fu X, Geisler M, Qi Y, Gao Z *et al.* 2021. A novel *miR167a-OsARF6-OsAUX3* module regulates grain length and weight in rice. *Molecular Plant* **14**: 1683–1698.

Qin Q, Li G, Jin L, Huang Y, Wang Y, Wei C, Xu Z, Yang Z, Wang H, Li Y. 2020. Auxin response factors (ARFs) differentially regulate rice antiviral immune response against rice dwarf virus. *PLoS Pathogens* **16**: e1009118.

Rhoades MW, Reinhart BJ, Lim LP, Burge CB, Bartel B, Bartel DP. 2002. Prediction of plant microRNA targets. *Cell* **110**: 513–520.

Rushton PJ, Somssich IE, Ringler P, Shen QJ. 2010. WRKY transcription factors. *Trends in Plant Science* **15**: 247–258.

Salvador-Guirao R, Hsing YI, San Segundo B. 2018. The polycistronic miR166k-166h positively regulates rice immunity via post-transcriptional control of *EIN2*. *Frontiers in Plant Science* **9**: 337.

Seo JK, Wu J, Lii Y, Li Y, Jin H. 2013. Contribution of small RNA pathway components in plant immunity. *Molecular Plant–Microbe Interactions* **26**: 617–625.

Shen C, Wang S, Bai Y, Wu Y, Zhang S, Chen M, Guilfoyle TJ, Wu P, Qi Y. 2010. Functional analysis of the structural domain of ARF proteins in rice (*Oryza sativa* L.). *Journal of Experimental Botany* **61**: 3971–3981.

Shen X, He J, Ping Y, Guo J, Hou N, Cao F, Li X, Geng D, Wang S, Chen P *et al.* 2022. The positive feedback regulatory loop of miR160-auxin response factor 17-HYPONASTIC LEAVES 1 mediates drought tolerance in apple trees. *Plant Physiology* **188**: 1686–1708.

Shimono M, Koga H, Akagi A, Hayashi N, Goto S, Sawada M, Kurihara T, Matsushita A, Sugano S, Jiang CJ *et al.* 2012. Rice WRKY45 plays important roles in fungal and bacterial disease resistance. *Molecular Plant Pathology* **13**: 83–94.

Shimono M, Sugano S, Nakayama A, Jiang CJ, Ono K, Toki S, Takatsuji H. 2007. Rice WRKY45 plays a crucial role in benzothiadiazole-inducible blast resistance. *Plant Cell* **19**: 2064–2076.

Sims K, Abedi-Samakush F, Szulc N, Macias Honti MG, Mattsson J. 2021. OsARF11 promotes growth, meristem, seed, and vein formation during rice plant development. *International Journal of Molecular Sciences* **22**: 4089.

Song X, Li Y, Cao X, Qi Y. 2019. MicroRNAs and their regulatory roles in plant-environment interactions. *Annual Review of Plant Biology* **70**: 489–525.

Talbot NJ. 2003. On the trail of a cereal killer: exploring the biology of *Magnaporthe grisea*. *Annual Review of Microbiology* **57**: 177–202.

Viana VE, Busanello C, da Maia LC, Pegoraro C, Costa de Oliveira A. 2018. Activation of rice WRKY transcription factors: an army of stress fighting soldiers? *Current Opinion in Plant Biology* **45**: 268–275.

Voinnet O. 2009. Origin, biogenesis, and activity of plant microRNAs. *Cell* **136**: 669–687.

Wang D, Pei K, Fu Y, Sun Z, Li S, Liu H, Tang K, Han B, Tao Y. 2007. Genome-wide analysis of the *auxin response factors* (ARF) gene family in rice (*Oryza sativa*). *Gene* **394**: 13–24.

Wang H, Jiao X, Kong X, Hamera S, Wu Y, Chen X, Fang R, Yan Y. 2016. A signaling cascade from miR444 to RDR1 in rice antiviral RNA silencing pathway. *Plant Physiology* **170**: 2365–2377.

Wang H, Li Y, Chern M, Zhu Y, Zhang LL, Lu JH, Li XP, Dang WQ, Ma XC, Yang ZR *et al.* 2021. Suppression of rice miR168 improves yield, flowering time and immunity. *Nature Plants* **7**: 129–136.

Wang H, Meng J, Peng X, Tang X, Zhou P, Xiang J, Deng X. 2015. Rice WRKY4 acts as a transcriptional activator mediating defense responses toward *Rhizoctonia solani*, the causing agent of rice sheath blight. *Plant Molecular Biology* **89**: 157–171.

Wang J, Zhou L, Shi H, Chern M, Yu H, Yi H, He M, Yin J, Zhu X, Li Y *et al.* 2018. A single transcription factor promotes both yield and immunity in rice. *Science* **361**: 1026–1028.

Wang Z, Xia Y, Lin S, Wang Y, Guo B, Song X, Ding S, Zheng L, Feng R, Chen S *et al.* 2018. Osa-miR164a targets *OsNAC60* and negatively regulates rice immunity against the blast fungus *Magnaporthe oryzae*. *The Plant Journal* **95**: 584–597.

Wu HJ, Wang ZM, Wang M, Wang XJ. 2013. Widespread long noncoding RNAs as endogenous target mimics for microRNAs in plants. *Plant Physiology* **161**: 1875–1884.

Wu J, Yang R, Yang Z, Yao S, Zhao S, Wang Y, Li P, Song X, Jin L, Zhou T *et al.* 2017. ROS accumulation and antiviral defence control by microRNA528 in rice. *Nature Plants* **3**: 16203.

Wu L, Zhang Q, Zhou H, Ni F, Wu X, Qi Y. 2009. Rice microRNA effector complexes and targets. *Plant Cell* **21**: 3421–3435.

Xiao S, Ellwood S, Calis O, Patrick E, Li T, Coleman M, Turner J. 2001. Broad-spectrum mildew resistance in *Arabidopsis thaliana* mediated by RPW8. *Science* **291**: 118–120.

Xie K, Minkenberg B, Yang Y. 2015. Boosting CRISPR/Cas9 multiplex editing capability with the endogenous tRNA-processing system. *Proceedings of the National Academy of Science, USA* **112**: 3570–3575.

Zhang L, Huang Y, Zheng Y, Liu X, Zhou S, Yang X, Liu S, Li Y, Li J, Zhao S *et al.* 2022. Osa-miR535 targets *SQUAMOSA promoter binding protein-like 4* to regulate blast disease resistance in rice. *The Plant Journal* **110**: 166–178.

Zhang LL, Li Y, Zheng YP, Wang H, Yang X, Chen JF, Zhou SX, Wang LF, Li XP, Ma XC *et al.* 2020. Expressing a target mimic of miR156fhl-3p enhances rice blast disease resistance without yield penalty by improving *SPL14* expression. *Frontiers in Genetics* **11**: 327.

Zhang S, Wang S, Xu Y, Yu C, Shen C, Qian Q, Geisler M, Jiang de A, Qi Y. 2015. The auxin response factor, OsARF19, controls rice leaf angles through positively regulating *OsGH3-5* and *OsBRI1*. *Plant, Cell & Environment* **38**: 638–654.

Zhang X, Bao Y, Shan D, Wang Z, Song X, Wang Z, Wang J, He L, Wu L, Zhang Z *et al.* 2018. *Magnaporthe oryzae* induces the expression of a microRNA to suppress the immune response in rice. *Plant Physiology* **177**: 352–368.

Zhao ZX, Feng Q, Cao XL, Zhu Y, Wang H, Chandran V, Fan J, Zhao JQ, Pu M, Li Y *et al.* 2020. *Osa-miR167d* facilitates infection of *Magnaporthe oryzae* in rice. *Journal of Integrative Plant Biology* **62**: 702–715.

Zhao ZX, Feng Q, Liu PQ, He XR, Zhao JH, Xu YJ, Zhang LL, Huang YY, Zhao JQ, Fan J *et al.* 2021. RPW8.1 enhances the ethylene-signaling pathway to feedback-attenuate its mediated cell death and disease resistance in *Arabidopsis*. *New Phytologist* **229**: 516–531.

Zhou SX, Zhu Y, Wang LF, Zheng YP, Chen JF, Li TT, Yang XM, Wang H, Li XP, Ma XC *et al.* 2020. *Osa-miR1873* fine-tunes rice immunity against *Magnaporthe oryzae* and yield traits. *Journal of Integrative Plant Biology* **62**: 1213–1226.

Supporting Information

Additional Supporting Information may be found online in the Supporting Information section at the end of the article.

Fig. S1 miR160a is responsive to the causative agents of the most serious rice diseases.

Fig. S2 miR160a targets *Auxin Response Factors* and mediates the cleavage of *ARF8*.

Fig. S3 miR160a and *ARF8* regulate broad-spectrum disease resistance in rice.

Fig. S4 The mutation sites of *Auxin Response Factors*.

Fig. S5 Transcriptomic analysis of genes differentially expressed in *arf8* and Nipponbare.

Fig. S6 Yeast one-hybrid assay for potential binding of ARF8 to the *WRKY45* promoter.

Fig. S7 Purified proteins used in electrophoretic mobility shift assay (EMSA) and the *in vitro* chromatin immunoprecipitation (ChIP)-quantitative polymerase chain reaction.

Fig. S8 Identification of *WRKY45* and *ARF8* double mutants (*w45*/*arf8*) and *WRKY45* single mutant (*w45*) transgenic plants.

Methods S1 RNA-seq analysis.

Methods S2 5′ RNA ligase-mediated rapid amplification of cDNA ends (5′ RLM-RACE).

Methods S3 Maltose-binding protein (MBP) fusion protein isolation.

Methods S4 Yeast one-hybrid assay.

Table S1 The sequence of gRNA used in this article for CRISPR CAS9 system.

Table S2 Primers used in this study.

Table S3 The sequences of probes used in electrophoretic mobility shift assay.

Table S4 Total expressed genes identified from the filtered RNA-seq data.

Table S5 Different expressed genes identified from the filtered RNA-seq data.

Table S6 Downregulated genes in *arf8*.

Table S7 Upregulated genes in *arf8*.

Please note: Wiley Blackwell are not responsible for the content or functionality of any Supporting Information supplied by the authors. Any queries (other than missing material) should be directed to the *New Phytologist* Central Office.